MCB Journals.ASM.org

LOXL4 Is Induced by Transforming Growth Factor β1 through Smad and JunB/Fra2 and Contributes to Vascular Matrix Remodeling

Oscar Busnadiego,[a] José González-Santamaría,[a] David Lagares,[b] Juan Guinea-Viniegra,[c] Cathy Pichol-Thievend,[c] Laurent Muller,[a] Fernando Rodríguez-Pascual[a]

Centro de Biología Molecular Severo Ochoa and Laboratorio Mixto Consejo Superior de Investigaciones Científicas/Fundación Renal Iñigo Alvarez de Toledo, Madrid, Spain[a]; Fundación Banco Bilbao Vizcaya-CNIO Cancer Cell Biology Program, Centro Nacional de Investigaciones Oncológicas, Madrid, Spain[b]; College de France, Center for Interdisciplinary Research in Biology, Paris, France[c]

Transforming growth factor β1 (TGF-β1) is a pleiotropic factor involved in the regulation of extracellular matrix (ECM) synthesis and remodeling. In search for novel genes mediating the action of TGF-β1 on vascular ECM, we identified the member of the lysyl oxidase family of matrix-remodeling enzymes, lysyl oxidase-like 4 (LOXL4), as a direct target of TGF-β1 in aortic endothelial cells, and we dissected the molecular mechanism of its induction. Deletion mapping and mutagenesis analysis of the LOXL4 promoter demonstrated the absolute requirement of a distal enhancer containing an activator protein 1 (AP-1) site and a Smad binding element for TGF-β1 to induce LOXL4 expression. Functional cooperation between Smad proteins and the AP-1 complex composed of JunB/Fra2 accounted for the action of TGF-β1, which involved the extracellular signal-regulated kinase (ERK)-dependent phosphorylation of Fra2. We furthermore provide evidence that LOXL4 was extracellularly secreted and significantly contributed to ECM deposition and assembly. These results suggest that TGF-β1-dependent expression of LOXL4 plays a role in vascular ECM homeostasis, contributing to vascular processes associated with ECM remodeling and fibrosis.

Transforming growth factor β (TGF-β) is a pleiotropic factor with important roles during embryonic development and in the regulation of tissue homeostasis (1). TGF-β responses initiate by binding to and activating specific type I and II kinase receptors. Signaling from activated receptors propagates by phosphorylation of cytoplasmic mediators belonging to the Smad family, which translocate to the nucleus, acting as transcription factors. In addition to the canonical Smad pathway, alternative, non-Smad pathways participate in TGF-β responses and serve as nodes for cross talk with, for example, the mitogen-activated protein kinase (MAPK) family (2).

TGF-β has been shown to be a key regulator of extracellular matrix (ECM) synthesis and remodeling. Specifically, TGF-β has the ability to induce the expression and deposition of ECM proteins, as well as to stimulate the production of protease inhibitors that prevent their enzymatic breakdown (3). TGF-β participates in the pathogenesis of many cardiovascular diseases, including hypertension, restenosis, atherosclerosis, cardiac hypertrophy, heart failure, and aortic aneurysms (4). A common observation in a number of vascular disorders is the alteration of the biomechanical properties, which is a consequence of increased ECM stiffness and subsequent loss of elasticity (5–7). Therefore, the ECM seems to be central to understand the contribution of TGF-β to the pathogenesis of vascular diseases.

Collagens and elastin, the main ECM components of the vascular matrix, are organized into supramolecular complexes forming fibers and network-like structures (8). The assembly of collagen fibrils and tropoelastin monomers is stabilized by the formation of covalent associations. Lysyl oxidases (LOX) constitute a family of enzymes which catalyze the conversion of lysine and hydroxylysine groups into highly reactive aldehydes, which eventually condense to form a variety of inter- and intrachain cross-linkages (9). To date, five LOX enzymes have been identified (LOX and LOX-like 1 to LOX-like 4), characterized by sharing the conserved C-terminal copper binding and catalytic domains and the unique N-terminal domains that determine individual roles. LOX family members are essential factors for the maturation of the ECM as evidenced in mouse models deficient in LOX and LOXL1, which show aortic malformations (10, 11). The precise functions and catalytic activities on elastin and collagen substrates of the remaining members of the LOX family (LOXL2 to -4) are not yet well understood.

In this work we identified the genes upregulated by TGF-β1 in bovine aortic endothelial cells, with particular emphasis on those associated with the ECM and therefore potentially involved in ECM homeostasis. We report LOXL4 as a direct target of TGF-β1 signaling and describe the characterization of the molecular mechanism utilized by TGF-β1 to induce its expression. We also provide evidence that LOXL4 is extracellularly secreted and significantly contributes to ECM deposition. These data suggest that TGF-β1-dependent expression of LOXL4 can play a role in vascular ECM homeostasis, with potential implications in vascular pathologies associated with matrix remodeling and fibrosis.

MATERIALS AND METHODS

Cell culture. Primary bovine aortic endothelial cells (BAEC) were isolated from thoracic aortas and maintained in culture using previously described methods (12). Mouse aortic endothelial cells (MAEC) were purchased from Angio-Proteomie (Boston, MA) and cultured according to the man-

Received 9 January 2013 Returned for modification 22 January 2013
Accepted 1 April 2013
Published ahead of print 9 April 2013
Address correspondence to Fernando Rodríguez-Pascual, frodriguez@cbm.uam.es.
Supplemental material for this article may be found at http://dx.doi.org/10.1128/MCB.00036-13.

doi:10.1128/MCB.00036-13

ufacturer's instructions. Smad3 knockout and wild-type embryonic fibroblasts (MEF) were isolated from newborn mice and kept in culture using standard procedures (13). Tetracycline (Tet)-inducible human embryonic kidney 293 (HEK 293) cells stably expressing LOXL4-green fluorescent protein (GFP) constructs were generated and maintained in culture according to protocols previously published (14).

RNA expression by quantitative PCR and microarray analysis. For RNA experiments, BAEC or MAEC were cultured in 100-mm cell culture dishes and treated with 5 ng/ml TGF-β1 (R&D Systems, Minneapolis, MN). Total RNA was isolated by guanidinium thiocyanate/phenol-chloroform extraction (15). cDNA was synthesized from 1 μg of RNA using an iScript cDNA synthesis kit, and quantitative PCR for the detection of LOX isoforms or Fra2 mRNA was performed using iQ SYBR green Supermix and specific primers (see Table S1 in the supplemental material) in a CFX96 thermocycler (Bio-Rad, Hercules, CA). Relative mRNA expression was determined using the glyceraldehyde 3-phosphate dehydrogenase gene as a housekeeping gene according to the $\Delta\Delta C_T$ method (16).

cDNA microarray analysis was carried out using a GeneChip bovine array (Affymetrix, Santa Clara, CA) containing 24,027 probe sets representing over 23,000 transcripts (including approximately 19,000 UniGene clusters). The purity and integrity of total RNA were checked with an RNA Bioanalyzer (Agilent 2100). RNA labeling, hybridization, scanning, and analysis were performed in the Genomics Unit of the Centro Nacional de Biotecnología (Madrid, Spain) according to the manufacturer's instructions. Genes showing statistically significant expression changes in response to TGF-β1 exposure were identified by using a cutoff value of 2.

Western blot analyses. For protein studies, bovine aortic endothelial or HEK 293 cells were cultured in 100-mm cell culture dishes and processed essentially as previously described (12). Briefly, cells were washed with phosphate-buffered saline (PBS) and lysed with 300 μl Tris-SDS buffer (60 mM Tris-HCl [pH 6.8], 2% sodium dodecyl sulfate [SDS]) to obtain total cell lysate. Protein concentrations were determined with the bicinchoninic acid (BCA) protein assay kit (Thermo Scientific, Rockford, IL). Equal amounts of protein (50 μg) were separated on 7.5% SDS-polyacrylamide gels, and fractioned proteins were transferred onto nitrocellulose membranes at 12 V for 50 min in a semidry Trans-Blot Turbo system (Bio-Rad). Membranes were blocked by incubation for 1 h with 3% bovine serum albumin (BSA) in PBS containing 0.5% Tween 20, and antigens were detected using specific primary antibodies (anti-LOXL4 [1:2,000, polyclonal, generated in our own laboratory by rabbit immunization with the C-terminal peptide ELSQEQEQRLRN, not conserved in the remaining LOX isoforms but highly homologous among bovine, mouse, and human LOXL4], anti-β-actin [1:20,000, monoclonal; Sigma], anti-Fra2 [1:1,000, rat antibody generated in our own laboratory using a histidine-tagged mouse full-length Fra2 protein], anti-Flag [1:2,000, mouse monoclonal from Sigma], anti-JunD [1:1,000, rabbit polyclonal; Santa Cruz], anti-JunB [1:1,000, rabbit polyclonal; Santa Cruz], anti-c-Jun [1:1,000, rabbit polyclonal; Santa Cruz], anti-extracellular signal-regulated kinase [anti-ERK] total [p44/42 MAPK] [1:2,000, rabbit polyclonal; Cell Signaling], anti-phospho-ERK [phospho-p44/42 MAPK, T202/T204] [1:1,000, rabbit polyclonal; Cell Signaling], and anti-GFP [1:2,000, mouse monoclonal; Roche]). Blots were then developed and quantified using corresponding IRDye 680- and IRDye 800-labeled secondary antibodies with the Odyssey infrared imaging system (Li-Cor).

5′ RACE. To define the transcription initiation site of the LOXL4 gene, 5′ rapid amplification of cDNA ends (5′ RACE) analysis was performed using the SMART RACE cDNA amplification kit (Clontech, Mountain View, CA). Briefly, total RNA from BAEC incubated with TGF-β1 was reverse transcribed in order to generate a first-strand cDNA suitable for 5′ RACE using SMART technology. A universal primer and a gene-specific primer (see Table S1 in the supplemental material) were then used for the generation of the 5′-end product. PCR fragments were analyzed by agarose electrophoresis and visualized with ethidium bromide staining. The resulting bands were excised from the gel, purified using the Geneclean Turbo kit (MP Biomedicals, Santa Ana, CA), and TA cloned into pCR2.1 (Life Technologies, Carlsbad, CA). A significant number of *Escherichia coli* colonies were picked, grown up, and analyzed by sequencing using M13 reverse and forward primers.

Construction of LOXL4 gene promoter reporter constructs and cell transfection. Analysis of LOXL4 gene transcriptional activity was performed by luciferase reporter gene studies using genomic fragments of the LOXL4 gene. Human LOXL4 promoter fragments were obtained by restriction cutting from clone RP11-34A14 on chromosome 10 containing complete LOXL4 gene (BACPAC resources; Children's Hospital Oakland Research Institute [CHORI]). Preliminary attempts to generate by PCR fragments of the LOXL4 promoter covering about 4 kb of 5′ flanking sequence and the complete exon 1 using bovine and mouse genomic DNAs were unsuccessful, likely due to the presence of a high GC sequence in the proximal promoter. Therefore, PCR assays were designed to generate the corresponding bovine and mouse LOXL4 promoter fragments upstream from the high-GC segment, and proximal promoter sequences were obtained by chemical synthesis (inserts in pBlueScript vector [Epoch Life Sciences, Missouri City, TX]) (see Table S2 in the supplemental material). Luciferase cassettes under the control of the LOXL4 promoter were generated by assembly of upstream PCR fragments and synthetic proximal sequences into pGL3 vector (Promega, Madison, WI) by standard cloning procedures. 5′ deletion constructs of the bovine LOXL4 promoter were generated by PCR and assembled into the luciferase reporter proximal promoter plasmid as described above. A distal fragment of the bovine LOXL4 promoter containing AP-1 and Smad binding elements (113 bp) was cloned in front of a cassette composed of a constitutive simian virus 40 (SV40) promoter fused to a luciferase gene (pGL3-Promoter; Promega) or assembled to the proximal promoter luciferase vector in order to analyze its potential enhancer capacity. Reporter luciferase constructs of the bp −3870 LOXL4 promoter with specific mutations in AP-1 and in Smad binding sites were generated by PCR-based site-directed mutagenesis as previously described (12). The AP-1 site TGAGTCA was replaced by GTAGTCA. Smad binding elements were mutated as follows: the SmadA CAGA was replaced by TAAT, and the SmadB GTCTG was changed to ATGTA. LOXL4 promoter constructs with a specific mutation in the Sp1 site (GGGGGCGGGG changed to GTTTTCGGGG) were obtained by chemical synthesis (Epoch Life Sciences). All constructs were verified by sequencing.

The vectors expressing the Smad3 and Smad7 transcription factors under the control of strong constitutive cytomegalovirus (CMV) promoters were kindly provided by Liliana Attisano (Toronto, Canada) and Aristidis Moustakas (Uppsala, Sweden), respectively. Mammalian expression vectors for Sp1 and Sp3 were kindly provided by Guntram Suske (Marburg, Germany). Mouse Fra2 cDNA was excised from pBabe-Fra2 plasmid and cloned into pcDNA3 (CMV promoter; Life Technologies) (17). A site-directed mutagenesis approach was used to generate a Fra2 expression vector with a C-terminal Flag tag (pcDNA3-Fra2-Flag) and, from this construct, Fra2-Flag phosphorylation mutants with inactivating mutations threonine to nonphosphorylatable alanine (T→A) and phosphomimetic mutations replacing threonine by glutamic acid (T→E) in residues T263 and T274 (see Table S3 in the supplemental material). Constructs for the overexpression of tethered JunB/Fra2, JunD/Fra2, and c-Jun/Fra2 dimers have been previously described (18).

DNA constructs were transiently transfected into BAEC, MAEC, and wild-type or Smad3 knockout mouse embryonic fibroblasts on 24-well plates (60 to 70% confluence), and promoter activity was estimated by luminometry as described previously, using the pRL-CMV plasmid (containing a *Renilla* luciferase gene under the control of the CMV promoter) for normalization purposes (12)

Comparative genomic DNA analysis was performed by using the Mulan multiple-alignment server (http://mulan.dcode.org) available at the National Center for Biotechnology Information DCODE server (ECR browser; http://www.dcode.org/) (19). LOXL4-orthologous sequences from *Homo sapiens*, *Mus musculus*, *Rattus norvegicus*, *Canis familiaris*, *Felis catus*, *Bos taurus*, *Pongo pygmaeus*, *Pan troglodytes*, and *Equus caballus*

were obtained from the ENSEMBL genome database (http://www.ensemble.org/). The CPGPlot program was used to detect CpG-rich regions that may correspond to potential CpG islands. The ClustalW2 program was used to align protein sequences from Fra2 and c-Fos orthologs in order to screen for evolutionary conserved MAPK phosphorylation sites (http://www.ebi.ac.uk).

ChIP. Chromatin immunoprecipitation (ChIP) experiments were performed using a commercially available kit (Pierce agarose ChIP kit; Thermo Fisher Scientific) according to the manufacturer's instructions. Briefly, cells were fixed with 1% formaldehyde (Calbiochem, La Jolla, CA) for 10 min at room temperature with swirling. Glycine was added to a final concentration of 0.125 M, and the incubation was continued for an additional 5 min. Cells were washed twice with ice-cold PBS, harvested by scraping, pelleted, and resuspended in 100 μl of lysis buffer containing protease inhibitors. Samples were centrifuged and the nuclear pellet resuspended in 100 μl of micrococcal nuclease (MNase) solution. Digestion proceeded for 15 min at 37°C with occasional mixing. Afterwards, the reaction was stopped, samples were centrifuged, and supernatants were saved as digested chromatin for immunoprecipitation. After removal of a control aliquot (input), samples were incubated at 4°C overnight with anti-Smad2/3 (mouse monoclonal; BD Transduction Laboratories, Franklin Lakes, NJ), anti-Fra2 (in-house, rat), or negative-control IgG. Protein A/G Plus agarose beads were then added, incubated for 1 h, and then extensively washed before chromatin was released by proteinase K digestion and DNA was further recovered using spin columns. Purified DNA was used for amplification of a region of 104 bp located at the upstream enhancer by real-time quantitative PCR (see Table S4 in the supplemental material). Quantities of target DNA in the ChIP and input samples were determined based on a standard curve and expressed as percentage of input after IgG background subtraction.

EMSA and oligonucleotide pulldown experiments. After different treatments, nuclear extracts were prepared according to a procedure described previously (20). Briefly, cell plates were washed once with ice-cold PBS and scraped in the same medium. Upon centrifugation, they were resuspended in 10 mM HEPES (pH 7.9), 10 mM KCl, 0.1 mM EDTA, 0.1 mM EGTA, 1 mM dithiothreitol (DTT), 0.5 mM phenylmethylsulfonyl fluoride, and 1 μg/ml each of leupeptin, aprotinin, and pepstatin A (Sigma). After 15 min of incubation on ice, Nonidet P-40 was added to a final concentration of 0.5% and cells were vortexed for 10 s. Then nuclei were sedimented by centrifugation for 5 min at 14,000 × *g*. The nuclear pellets were extracted by shaking on ice for 30 min in 20 mM HEPES (pH 7.9), 400 mM NaCl, 1 mM EDTA, 1 mM EGTA, 1 mM DTT, and protease inhibitors as described above. After centrifugation, nuclear debris was discarded by centrifugation at 14,000 × *g* for 5 min, and nuclear extracts were stored at −80°C. Protein content was determined using the Bradford method (Bio-Rad). Constructs for bacterial recombinant expression of the glutathione *S*-transferase (GST) fusion proteins GST-Smad2, GST-Smad3, and GST-Smad4 were kindly provided by Liliana Attisano (Toronto, Canada). Fusion proteins were expressed in *E. coli* and purified as described previously (12). JunB/Fra2 forced dimers, wild type or with mutations in residues T263 and T274, were prepared *in vitro* using the TNT rabbit reticulocyte coupled transcription-translation system (Promega). JunB/Fra2 protein expression was checked by Western blot analysis using anti-JunB antibody.

Electrophoretic mobility shift assays (EMSA) with nuclear extracts (4 μg), purified GST fusion forms (0.1 to 1 μg), or equivalent amounts of *in vitro*-synthesized proteins were performed as described previously using infrared-labeled oligonucleotides for the AP-1 or the Smad binding sites (see Table S5 in the supplemental material) (12). Free oligonucleotides and DNA-protein complexes were visualized with the Odyssey infrared imaging system (Li-Cor). For competition experiments, unlabeled oligonucleotides corresponding to wild-type Smad and AP-1 binding sites, or including specific mutations, were added to the incubation mixture in a 1- to 100-fold excess.

Oligonucleotide pulldown experiments were designed in order to identify and characterize proteins interacting with the DNA sequence containing the AP-1 and Smad binding sites. 5′-biotinylated wild-type and mutated AP-1/SmadB DNA fragments corresponding to positions −3866/−3754 were generated by PCR using the corresponding 5′-biotinylated forward primer and wild-type and mutated reverse primers (see Table S4 in the supplemental material), purified using Geneclean (Turbo kit MP Biomedicals), and verified by electrophoresis and ethidium bromide staining. For the reaction, 100 μg of nuclear extracts from bovine aortic endothelial cells incubated with or without TGF-β1 was incubated for 20 min at 4°C in a volume of 100 μl of binding buffer [10 mM Tris-HCl (pH 7.4), 50 mM NaCl, 1 mM $MgCl_2$, 5 mM DTT, and 5% glycerol and containing 0.02 mg/ml of poly(dI-dC) (General Electric, Little Chalfont, United Kingdom)] with 5′-biotinylated wild-type and mutated oligonucleotides. Afterwards, 50 μl of SoftLink soft release avidin resin (Promega; 1:1 slurry, equilibrated according to the manufacturer's instructions) was added and the mixture further incubated for 1 h at 4°C with occasional shaking. Beads were then washed five times with 500 μl of binding buffer without poly(dI-dC). Retained proteins were finally eluted from the beads by addition of 50 μl Laemmli buffer and centrifugation at 14,000 × *g* for 15 min, fractioned by SDS-PAGE, and visualized by Coomassie blue staining.

Bands corresponding to candidate proteins were dissected and gel pieces digested *in situ* with sequencing-grade trypsin (Promega) as previously described (21). Mixtures of proteolytically generated peptides were analyzed by reverse-phase liquid chromatography–tandem mass spectrometry (RP-LC-MS/MS) in an Agilent 1100 system coupled to a linear ion trap LTQ-Velos mass spectrometer (Thermo Fisher Scientific). The peptides were separated using a 0.18- by 150-mm Bio-Basic C_{18} RP column (Thermo Fisher Scientific) operating at 1.8 μl/min. Peptides were eluted using a 35-min gradient from 5 to 40% solvent (solvent A, 0.1% formic acid in water; solvent B, 0.1% formic acid and 80% acetonitrile in water). Electrospray ionization (ESI) was done using a microspray "metal needle kit" interface (Thermo Fisher Scientific). Peptides were detected in survey scans from 400 to 1,600 amu (1 microscan), followed by five data-dependent MS/MS scans (Top 5), using an isolation width of 2 U (in mass-to-charge ratio units), a normalized collision energy of 35%, and dynamic exclusion applied during 30-s periods. Peptide identification from raw data was carried out with the SEQUEST algorithm (Proteome Discoverer 1.2; Thermo Fisher Scientific) using the *Bos taurus* UniProt database. The following constraints were used for the searches: tryptic cleavage after Arg and Lys, up to two missed cleavage sites, and tolerances of 1 Da for precursor ions and 0.8 Da for MS/MS fragment ions. The searches were performed allowing optional Met oxidation and Cys carbamidomethylation. Searching against a decoy database (interpreted decoy approach) was performed using a false discovery rate of <0.01. The complete proteomic analysis was carried out in the Centro de Biología Molecular Severo Ochoa Protein Chemistry Unit, a member of ProteoRed network (www.proteored.org).

GST-Fra2 pulldown assays. Mouse Fra2 cDNA sequence was amplified from plasmid pBabe-Fra2 with primers containing adequate restriction sites for cloning into the pGEX-2T vector (GE Healthcare, Little Chalfont, Buckinghamshire, United Kingdom) (see Table S6 in the supplemental material). Specific mutations in residues T263 and T274 were introduced by site-directed mutagenesis using primers shown in Table S3 in the supplemental material. Fusion proteins were expressed in *E. coli* and purified as described previously (12). For pulldown experiments, equivalent amounts of GST-Fra2 beads were incubated with total extracts from bovine aortic endothelial cells for 2 h at room temperature with rocking. The beads were then washed four times with PBS and then resuspended in Laemmli buffer for SDS-PAGE and Western blot analysis of endogenous JunB and recombinant Fra2.

Adenoviral infection and siRNA-mediated inhibition of gene expression. Recombinant-deficient human adenovirus type 5 (dE1/E3) overexpressing a dominant negative form of AP-1 (Adv-TAM67) and empty vector adenovirus (Adv-Null) were purchased from Vector Biolabs

(Philadelphia, PA). Mouse Fra2 and bovine LOXL4 cDNA (the former excised from pcDNA3-Fra2 and the latter generated by reverse transcription coupled to PCR using total RNA from TGF-β1-incubated bovine aortic endothelial cells) were cloned into a suitable shuttle vector to generate adenoviral constructs for mammalian overexpression (Vector Biolabs). Adenoviruses were amplified using embryonic kidney cell line HEK 293. Briefly, HEK 293 cells were cultured until the monolayer was 90% confluent and then infected with cytopathic levels of adenoviruses for 48 h. For purification of adenoviruses, infected cells and supernatants were taken and centrifuged at 1,000 × *g* for 5 min. Supernatants were discarded, and cell pellets were lysed with three freezing-thawing cycles to release virus particles. The viruses were then purified using the Adeno-X Maxi purification kit from Clontech (Mountain View, CA) according to the manufacturer's instructions. Virion concentrations were determined using the Adeno-X-Rapid titer kit from Clontech, and viral stocks were stored in aliquots at −80°C. For adenoviral infection of primary bovine aortic endothelial cells, these were seeded in 100-mm culture dishes and exposed to adenoviral constructs for 24 h. Cells were then washed and incubated in serum-free medium for an additional 24-h period. In some experiments, infected cells were transfected with DNA plasmid during this 24-h period. Cells were then finally stimulated with TGF-β1 or left untreated as indicated.

Specific small interfering RNAs (siRNAs) for the inhibition of the expression of bovine Fra2, c-Jun, JunB, and JunD and a nontargeting control were purchased from Ambion (Silencer Select siRNA; Life Technologies) (see Table S7 in the supplemental material). Cell transfections were performed in 6-well plates as described above.

Immunofluorescence microscopy. Fluorescence microscopy was performed as previously described (22). Briefly, primary bovine aortic endothelial cells were seeded onto 24-well plates containing 10-mm-diameter glass coverslips. After the corresponding treatment, cells were fixed with 4% paraformaldehyde in PBS for 10 min and then permeabilized with 0.2% Triton X-100 in PBS for 5 min at room temperature. Cells were washed with PBS, blocked with 1% BSA in PBS for 1 h, and then incubated overnight at 4°C with primary antibodies (anti-Fra2 [1:200, rat antibody described above], anti-GFP [1:200, mouse monoclonal from Roche], and anticalnexin [endoplasmic reticulum [ER] marker, 1:200, rabbit polyclonal; Stressgen, San Diego, CA), followed by the corresponding fluorescent secondary antibodies. For collagen IV staining (anti-collagen IV [1:200, rabbit polyclonal; Novotec, Lyon, France), cells were fixed with cold methanol for 5 min and blocked with 10% goat serum for 20 min after three washes with PBS before the incubation with the antibody. Nuclear staining was performed with DAPI (4′,6′-diamidino-2-phenylindole) (Sigma). Cell fluorescence was visualized by microscopy with a Nikon Eclipse T2000U (Nikon, Amstelveen, The Netherlands) or an LSM710 laser confocal microscope (Carl Zeiss, Overkochen, Germany).

Mammalian expression of recombinant LOXL4-GFP isoforms. To study subcellular localization and potential extracellular secretion of LOXL4, we generated constructs for the overexpression of a fusion protein of bovine LOXL4 and green fluorescent protein (LOXL4-GFP). For that purpose, LOXL4 cDNA was cloned into pEGFP-N1 vector (Life Technologies) to yield full-length LOXL4-GFP. Deletion mutants from this construct lacking the scavenger receptor cysteine-rich (SRCR) domains and the C-terminal catalytic region were generated by site-directed mutagenesis (see oligonucleotide sequences in Table S8 in the supplemental material). These constructs were used for transient transfection in primary aortic endothelial cells as described above. To generate stable transfectants of HEK 293 cells overexpressing LOXL4-GFP isoforms, LOXL4-GFP fragments were cloned into the pcDNA5/FRT/TO vector (Life Technologies) to give pcDNA5/FRT/TO/LOXL4-GFP constructs. These constructs were then cotransfected with the Flp recombinase expression plasmid pOG44 into the Flp-In T-Rex 293 cell line (Life Technologies). Cells of this line stably express the tetracycline (Tet) repressor and contain a single integrated Flp recombination target (FRT) site. Flp recombinase expression from the pOG44 vector mediates insertion of pCDNA5/FRT/TO-based constructs into the genome at the integrated FRT site through site-specific DNA recombination. After 48 h, cells were selected with hygromycin B, and clones appeared after 10 to 15 days. Isogenic pooled clones were expanded and used for experiments involving induction by the Tet analog doxycycline (Dox). Expression of LOXL4-GFP chimeras upon Dox incubation was checked by Western blotting using anti-GFP antibodies as described above.

Detection of LOXL4 in the extracellular medium. The release of LOXL4 to the extracellular medium was investigated in HEK 293 cells overexpressing LOXL4-GFP isoforms. Cells were seeded on 100-mm culture dishes. When 90% confluence was reached, they were incubated with 5 ml of serum-free medium containing doxycycline (1 μg/ml) for 48 h. Cell supernatants were collected, centrifuged at 100,000 × *g* for 1 h at 4°C, and then concentrated down to 100 μl using Amicon ultracentrifugal filters (Ultracel-10K; Millipore, Billerica, MA) and further immunoprecipitated by incubation overnight at 4°C with anti-GFP antibody. After addition of 50 μl of SoftLink soft release avidin resin (Promega), samples were incubated for 1 h at 4°C. Beads were then washed five times with buffer and retained proteins eluted out from the beads by adding Laemmli buffer. Supernatants were subjected to SDS-PAGE, fractioned proteins transferred to nitrocellulose membranes, and GFP-immunoreactive bands detected by Western blotting as described above.

***In vitro* collagen remodeling and lysyl oxidase activity assays.** Conditioned medium from primary bovine aortic endothelial cells incubated with or without TGF-β1 or infected with Adv-LOXL4 or control Adv-Null was concentrated by means of Amicon ultracentrifugal devices as described above. Type I collagen solution (2 mg/ml) was mixed with concentrated medium and incubated at 37°C for 30 min. Additional medium was added on top of the gelled collagen for further incubation at 37°C for 16 h. The gel was analyzed under confocal reflection microscopy in an LSM710 laser confocal microscope (Carl Zeiss) as previously described (23).

Cell supernatants were also assayed for lysyl oxidase activity using diaminopentane and Amplex red as previously described (24). In a typical assay, samples of 100 μl of concentrated medium were mixed with the reaction mixture containing 10 mM diaminopentane, 10 μM Amplex red, and 1 U horseradish peroxidase in 1.2 M urea–0.05 M sodium borate (pH 8.2) in the presence or absence of 0.5 mM β-aminopropionitrile (BAPN), an active-site inhibitor of lysyl oxidases. H_2O_2 release was measured every 15 min for a total period of 24 h at excitation and emission wavelengths of 525 and 580 to 640 nm, respectively, on a Glomax multidetection system (Promega). Enzyme activities were expressed as fluorescence values, corrected for background levels of H_2O_2 release determined in the reaction mixture supplemented with BAPN. Recombinant human LOXL2, used as a positive control for lysyl oxidase activity, was purchased from R&D Systems.

Statistical analysis. Experimental data were analyzed using the unpaired Student *t* test in the case of normal distribution of data or using nonparametric tests as appropriate. The *P* values obtained are indicated in the figure legends when statistically significant ($P < 0.05$).

Microarray data accession number. The microarray data are publicly available at the National Center for Biotechnology Information Gene Expression Omnibus (http://www.ncbi.nlm.nih.gov/geo/) under accession number GSE42932.

RESULTS

TGF-β1 strongly induces LOXL4 expression in aortic endothelial cells through Smad and AP-1. In order to gain insight about the potential ECM-related TGF-β1 target genes in the cardiovascular system, we profiled mRNAs from bovine aortic endothelial cells under basal conditions and incubated with TGF-β1 for 24 h. Comparing with control cells, it was found that TGF-β1 exerted a profound effect on global expression, with more than 500 genes upregulated under our experimental conditions (GEO accession

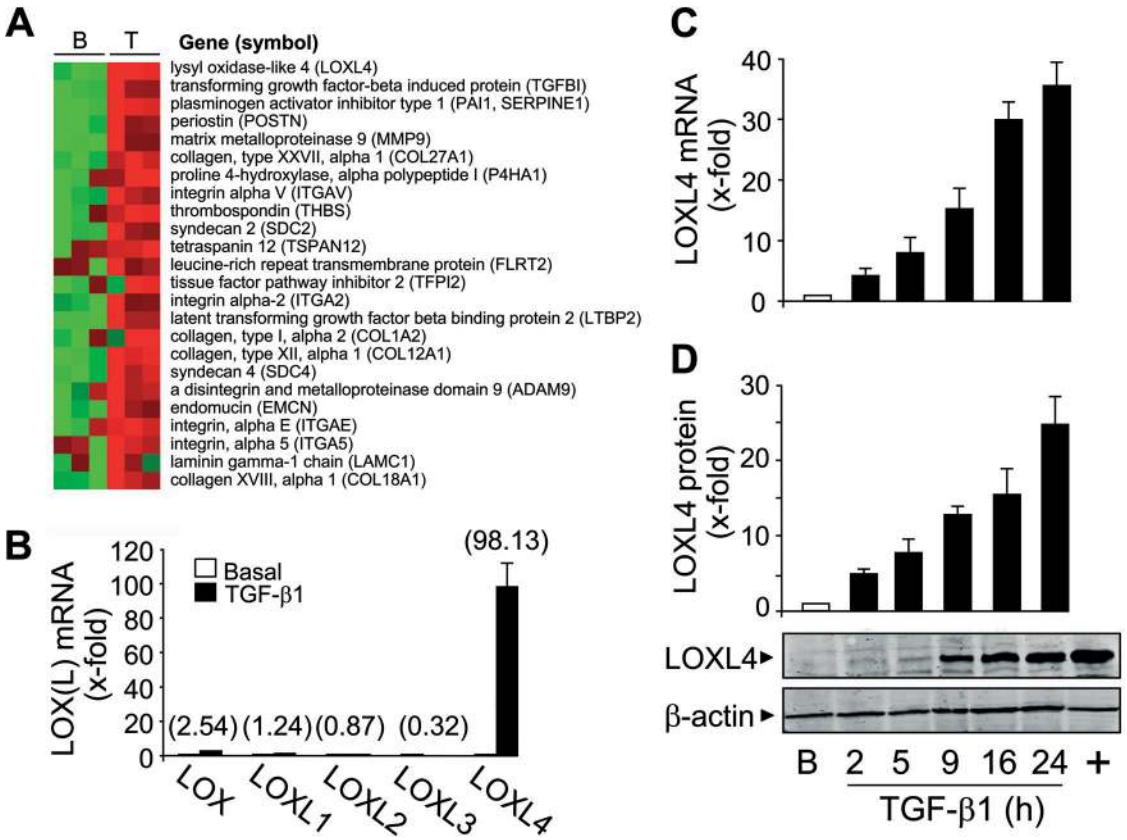

FIG 1 LOXL4 is a TGF-β1 target gene in aortic endothelial cells. (A) Panel of ECM-related genes showing significant expression changes (fold change, >2) upon 24 h of TGF-β1 (5 ng/ml) treatment, identified by genome-wide expression. (B) Quantitative PCR of LOX gene family members (LOX and LOXL1 to -4) in TGF-β1-stimulated BAEC. Values above the bars in parentheses indicate the induction rates with respect to basal levels. (C) LOXL4 mRNA expression as a function of TGF-β1 incubation time as assessed by quantitative PCR. (D) Time-dependent effect of TGF-β1 on LOXL4 protein (representative Western blotting and densitometric analysis of the LOXL4/β-actin signal). +, positive control of cells infected with LOXL4 adenovirus. Values are represented as fold induction with respect to basal values (means ± standard errors of the means [SEM]; $n = 3$).

number GSE42932). A significant number of genes positioned at the top of the list can be classified as ECM-related targets, including several collagen isoforms as well as collagen-modifying enzymes (Fig. 1A). A candidate TGF-β1 target gene, that for lysyl oxidase-like isoform 4 (LOXL4), attracted our attention as it showed the strongest induction, in addition to its relevance for ECM synthesis and remodeling. Analysis of the ability of TGF-β1 to modulate the expression of lysyl oxidase family members revealed that only LOXL4 and, to a lesser extent, the canonical LOX were upregulated in this cell model (Fig. 1B). Careful examination of the time course response of the LOXL4 gene to TGF-β1 showed that mRNA and protein begin to accumulate at as early as 2 h of incubation with the cytokine, indicating that LOXL4 might be a direct target for the action of TGF-β1 in the endothelium (Fig. 1C and D).

To elucidate the transcriptional mechanism for the control of LOXL4 expression by TGF-β1, we isolated a genomic fragment of the promoter of the bovine gene. Conflicting reports exist on the position of the transcriptional start site and therefore on the precise location of the promoter in the human gene (25, 26). Additionally, experimental evidence about the site(s) for the initiation of transcription in the bovine model has not been reported. Therefore, we first endeavored to identify the transcription initiation sites in the bovine LOXL4 gene by 5′ rapid amplification of cDNA ends (5′ RACE). A major 5′ RACE product was obtained and sequenced, yielding several start sites tightly clustering around the annotated site for the initiation of transcription located 121 nucleotides upstream of the translation initiation codon ATG (see Fig. S1 in the supplemental material). Based on this finding, a genomic fragment of approximately 4 kb (−3870/+87) including the 5′ flanking sequence and complete exon 1 was generated and cloned in front of a luciferase reporter gene to study the effect of TGF-β1. In a set of preliminary experiments, we tested this fragment and also a pair of truncated constructs of 2.2 and 0.3 kb. As shown in Fig. S2 in the supplemental material, while the activity of these truncated promoter fragments was not significantly modified by TGF-β1 incubation, the cytokine induced a potent increase in luciferase activity (5- to 6-fold at 24 h) in cells transfected with the longest, 4-kb construct. These results indicate that a promoter region between bp −3870 and −2266 contains the critical elements to mediate the transcriptional activation of the gene.

We screened the bp −3870/−2266 promoter region for putative binding sites for Smad and AP-1 transcription factors, both of which have been described to be important for the effect of TGF-β1 on gene expression (12, 27, 28). An upstream AP-1 consensus site (TGAGTCA) and several elements identical or similar to the Smad consensus sequence (CAGAC), either alone or in a palindromic form, were identified by *in silico* analysis (see Fig. S3

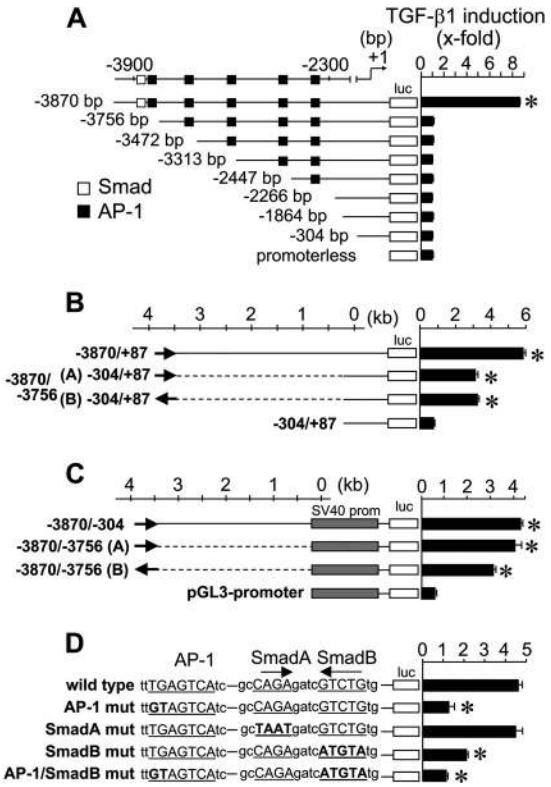

FIG 2 Mapping of TGF-β1-responsive elements within the LOXL4 promoter. (A) TGF-β1-dependent activity of luciferase constructs driven by 5′ deletion fragments of the LOXL4 promoter from bp −3870 to −304 transfected into BAEC. A schematic representation of the bp −3900/−2300 promoter sequence shows the position of putative AP-1 and Smad sites (white and black boxes, respectively). (B and C) The −3870/−3756 promoter fragment is sufficient to confer TGF-β1 responsiveness to its cognate proximal promoter (−304/+87) (B) and to a viral SV40 promoter (pGL3-Promoter) (C) in an orientation-independent manner. (D) Specific point mutations in the bp −3870/+87 LOXL4 promoter construct that alter Smad and AP-1 elements as indicated were introduced and their TGF-β1 inducibility measured by luminometry. TGF-β1 induction rates are expressed as mean ± SEM ($n = 3$). *, $P < 0.05$ versus promoterless construct (A) versus −304/+87 proximal LOXL4 promoter (B), versus pGL3-Promoter (C), or versus the wild type (D), in the absence of TGF-β1.

in the supplemental material). Based on the location of these putative regulatory elements, we generated a set of 5′ deletion luciferase constructs and tested their inducibility by TGF-β1. As shown in Fig. 2A, the TGF-β1 response observed with the −3870/+87 fragment was eliminated as soon as a short segment of 113 bp containing putative AP-1 and Smad elements was removed. In fact, this fragment can be considered an enhancer, as it is able to confer TGF-β1 responsiveness to a core promoter in a manner that is independent of its orientation and distance relative to the RNA start site, as shown in experiments with constructs generated in the context of its cognate proximal promoter and of the viral SV40 promoter (Fig. 2B and C). In order to assess the relevance of the AP-1 and Smad elements identified in this enhancer region, we generated full promoter constructs (bp −3870/+87) with specific mutations in these sites (AP-1, SmadA, and SmadB) and tested their activity upon TGF-β1 stimulation. As shown also in Fig. 2D, the disruption of the AP-1 element and the downstream Smad site, the consensus SmadB, either in individually or combined in the same construct, caused a significant reduction in their ability to respond to TGF-β1. In contrast, the specific mutation of the upstream Smad-like site (SmadA) did not show any significant effect.

Multiple-sequence alignment analysis is a powerful approach for identifying functional regulatory elements, such as exons or enhancers. We used the Mulan multiple-alignment server (http://mulan.dcode.org) to analyze the promoter regions of several mammalian orthologs of LOXL4 in order to evaluate the relevance of the DNA elements identified in the present study and also to screen for an additional control region(s) (19). As shown in Fig. 3A, at least three well-conserved regions were identified across these genomes, namely, a short stretch at the proximal promoter, a broader region in the central portion of the promoter fragment used for comparison, and finally, an upstream region partially overlapping the enhancer involved in the TGF-β1 induction. Surprisingly, rodent genomes differed from the rest of mammalian genomes compared in this study, as they did not show significant homology in the upstream enhancer. Careful examination of the sequence of this DNA segment revealed that the consensus AP-1 site is not present in the equivalent regions from rat and mouse (Fig. 3B), an observation that predicts that the LOXL4 gene may not respond to TGF-β1 in these mammalian species. To test this hypothesis, the corresponding fragments of human and mouse LOXL4 promoters were isolated and fused to a luciferase reporter for analysis of their TGF-β-dependent transcriptional activity in BAEC and MAEC. As shown also in Fig. 3C, human and bovine LOXL4 promoters displayed significant TGF-β1 inducibility in both bovine and mouse cells. In contrast, the construct containing the mouse LOXL4 promoter was unresponsive to TGF-β1 in both bovine and mouse endothelial cells. Accordingly, LOXL4 gene expression was not altered by TGF-β1 in MAEC, whereas was highly upregulated in BAEC (Fig. 3D). These results are consistent with the analysis of conserved regions, and altogether the results underscore the contribution of the AP-1 and Smad elements within this enhancer region to the induction of LOXL4 expression by TGF-β1.

The well-conserved proximal promoter of the LOXL4 gene lacks a TATA box, but it contains a GC-rich region that may correspond to a potential CpG island. Using the CPGPlot program (http://www.ebi.ac.uk), analysis of the proximal LOXL4 promoter from bp −307 to +87 revealed a CpG island that lies between bp −260 and +29 (see Fig. S4A in the supplemental material). Sp1 is a ubiquitous transcription factor that binds GC-rich sequences that are present in many CpG islands, and it is reported to prevent their methylation (29). A consensus Sp1 site (GGGGGCGGGG) has been also identified in the CpG island of the LOXL4 proximal promoter (see Fig. S4A in the supplemental material). Site-directed mutagenesis of this putative Sp1 binding site strongly reduced the basal activity of LOXL4 promoter without significantly affecting the induction by TGF-β1 (see Fig. S4B in the supplemental material). Accordingly, the overexpression of Sp1 family members Sp1 and Sp3 increased both basal and TGF-β1-stimulated promoter activity (see Fig. S4C in the supplemental material), indicating that the proximal promoter importantly contributes to the basal transcription machinery but seems to be dispensable in the induction by TGF-β.

Smad and JunB/Fra2 transcription factors contribute to TGF-β1 induction of the LOXL4 gene. TGF-β regulates gene expression through Smad-dependent and -independent pathways

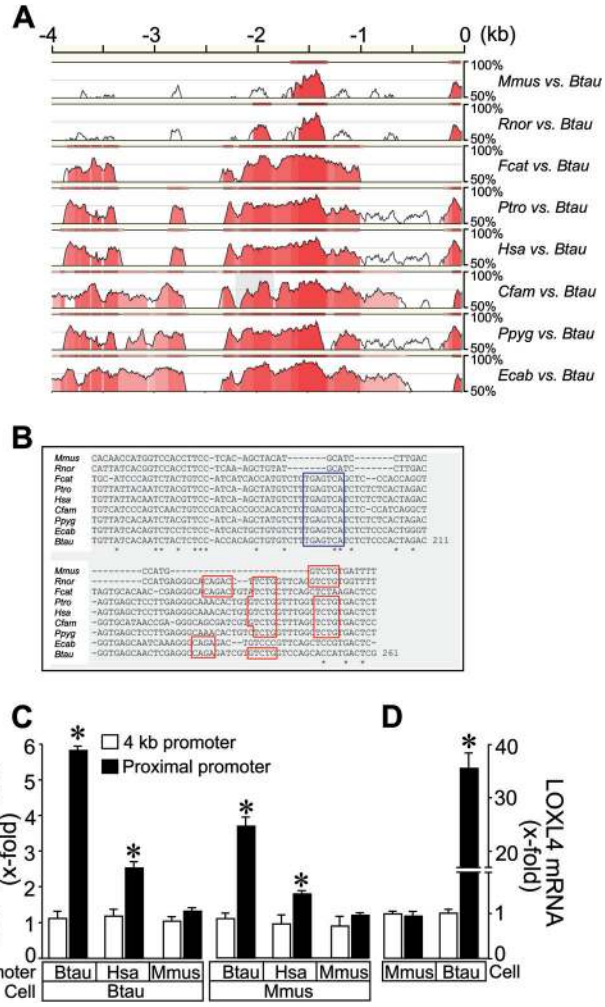

FIG 3 Analysis of conserved regions in the LOXL4 promoter across mammalian genomes. (A) Comparative genomic analysis of the promoter regions of several mammalian LOXL4 orthologs (Mulan multiple-alignment engine). The graphical representation shows stacked-pairwise conservation profiles for the 4-kb promoter region of the LOXL4 gene between the indicated species and the reference bovine sequence. The color intensity of a conserved region depends on the number of different species that contain the region (the darker the color, the more conserved species). Only evolutionarily conserved regions (ECR) present in at least six out of eight total secondary species are highlighted in the alignment. Note that sequence corresponding to proximal promoter from cat was not available in the ENSEMBL database. (B) Multiple-sequence alignment of the most upstream ECR, showing the locations of the AP-1 site (blue) and Smad binding elements (red). (C) TGF-β1 inducibility of bovine, human, and mouse 4-kb and proximal LOXL4 promoter luciferase constructs transfected into BAEC (Btau) and MAEC (Mmus). (D) Effect of TGF-β1 on LOXL4 mRNA expression in BAEC and MAEC as assessed by quantitative PCR. Values are represented as fold induction with respect to basal levels in the absence of TGF-β1 (mean ± SEM; $n = 3$). *, $P < 0.05$ versus the corresponding proximal promoter for luciferase activity (C) or versus the basal value for mRNA expression (D).

(30). To investigate the role of Smad family members in the mechanism of LOXL4 upregulation by TGF-β1, the activating Smad3 and the inhibitory Smad7 were overexpressed in BAEC and their effect on LOXL4 promoter activity analyzed in luciferase assays. Figure 4A shows that Smad3 potentiated, whereas Smad7 significantly reduced, both basal and TGF-β1-induced promoter activity. The implication of Smad3 was further confirmed by experiments with mouse embryonic fibroblasts (MEF) isolated from wild-type and Smad3 knockout embryos. As shown also in Fig. 4B, TGF-β1 activated the LOXL4 promoter in transfected wild-type MEF, whereas it showed no effect on Smad3 knockout cells. TGF-β1-mediated induction of the LOXL4 promoter was recovered in these cells upon reintroduction of Smad3.

On the other hand, the implication of AP-1 members was investigated by adenovirus-mediated overexpression of a dominant negative form of AP-1 (TAM67) that binds to DNA but is not able to transactivate (31). TAM67 dose dependently inhibited the induction of LOXL4 expression by TGF-β1 at the levels of both mRNA and promoter activity (Fig. 4C and D).

EMSA and ChIP experiments were performed to detect and characterize protein-DNA complexes at the LOXL4 promoter. EMSA with nuclear extracts from cells under basal conditions showed an AP-1 binding activity that was significantly increased upon incubation with TGF-β1 (see Fig. S5A and B in the supplemental material). The binding to this complex was competed out by an excess of unlabeled AP-1 oligonucleotide but not by a mutated one. Smad proteins bind to Smad sites with low affinity, and this feature makes their detection by EMSA difficult (32). ChIP using a specific Smad2/3 antibody successfully revealed the recruitment of Smad factors to the enhancer region within the LOXL4 promoter in a TGF-β1-dependent manner (see Fig. S5C in the supplemental material). Smad binding was further confirmed by EMSA with the use of recombinant proteins. Recombinant Smad4 and, to a lesser extent, Smad3 displayed strong binding activity to a Smad probe (see Fig. S5D in the supplemental material). In agreement with site-specific mutagenesis experiments, a wild-type Smad probe or a probe with a specific mutation in the Smad-like site, SmadA, efficiently competed out the binding observed to recombinant Smad4 compared with a probe mutated in the consensus SmadB (see Fig. S5E and F in the supplemental material).

In an effort to identify the proteins involved in the regulation of LOXL4 expression by TGF-β1, a DNA pulldown assay was employed to isolate proteins that specifically and differentially bind to a DNA sequence derived from the upstream enhancer. 5′-biotinylated wild-type and mutated AP-1/SmadB DNA fragments corresponding to positions −3870/−3756 were exposed to nuclear extracts from BAEC incubated with or without TGF-β1, and DNA-bound proteins were separated by SDS-PAGE and visualized by Coomassie blue staining (see Fig. S6A in the supplemental material). A protein band of approximately 35 kDa was significantly enriched in samples obtained from TGF-β1-treated cells and incubated with the wild-type oligonucleotide compared with those incubated with the mutant DNA probe or isolated from control cells. SEQUEST searches of LC-MS analyses of tryptic peptides from the excised band showed that one of the proteins identified corresponded to a member of the AP-1 family, FOS-like antigen 2 (FOSL2) or Fra2 (see Fig. S6B and C in the supplemental material).

Fra2 has recently evolved as an extremely interesting factor in the context of vascular ECM remodeling and fibrosis (33–36). In order to confirm the implication of Fra2 in the upregulation of LOXL4 expression, we performed gain- and loss-of-function experiments. Adenovirus-mediated overexpression of Fra2 potentiated TGF-β1-induced LOXL4 expression at the level of promoter activity and protein (Fig. 5A). Fra2 overexpression also associated with its binding to the enhancer region within the LOXL4 pro-

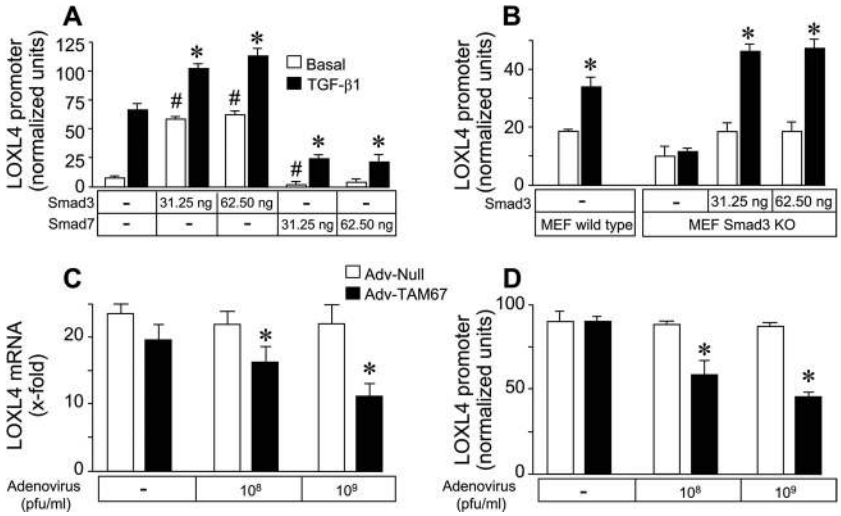

FIG 4 Involvement of Smad and AP-1 transcription factors in the effect of TGF-β1 on LOXL4 expression. (A) Luciferase activity of LOXL4 promoter luciferase constructs cotransfected with increasing amounts of Smad3 or Smad7 overexpression plasmids. (B) Wild-type and Smad3 knockout (KO) mouse embryonic fibroblasts (MEF) were transfected with the LOXL4 promoter together with Smad3 plasmid. (C and D) Effect of adenovirus-mediated overexpression of the dominant negative form of AP-1, TAM67 (10^8 to 10^9 PFU/ml) on TGF-β1-mediated induction of LOXL4 mRNA (C) and promoter activity (D). Values are represented as normalized units for luciferase activity and as fold induction with respect to basal values for mRNA expression (mean ± SEM; $n = 3$). *, $P < 0.05$ versus pcDNA3 empty vector (−) (A and B, right panel), versus basal levels in the absence of TGF-β1 stimulation (B, left panel), or versus empty vector null adenovirus (C and D).

moter as assessed by ChIP (validation of overexpression by adenoviral Fra2 and ChIP experiments is shown in Fig. S7A and B in the supplemental material). Conversely, specific silencing of endogenous Fra2 by siRNA technology significantly diminished the level of induction of LOXL4 expression by TGF-β1 (Fig. 5B) (validation of silencing by siRNA Fra2 is shown in Fig. S7C in the supplemental material). Proteins belonging to the AP-1 family bind DNA as obligate homo- or heterodimers. While Jun members can dimerize with each other and with Fos proteins, the members of the Fos subfamily, c-Fos, FosB, and Fra1 and Fra2, cannot form homodimers (37). To identify the Jun partner that dimerizes with Fra2 in TGF-β1-mediated activation of LOXL4 expression, we took advantage of the existence of tethered AP-1 dimers, including JunB/Fra2, JunD/Fra2, and c-Jun/Fra2, with AP-1 molecules joined via a flexible polypeptide tether to force specific pairing (18). As shown in Fig. 5C, overexpression of forced JunB/Fra2 dimer resulted in a potentiation of TGF-β1-induced promoter activity, while Fra2/JunD and c-Jun/Fra2 did not show any significant effect, compared with empty vector (validation of the overexpression of AP-1 dimers by anti-Flag Western blotting is shown in Fig. S7D in the supplemental material). The involvement of JunB was further confirmed by siRNA experiments. Specific downregulation of JunB expression resulted in a significant reduction of the effect of TGF-β1 on LOXL4 promoter activity, whereas the silencing of JunD and c-Jun did not have a significant effect (Fig. 5D) (validation of silencing of Jun proteins by siRNA is shown in Fig. S7E in the supplemental material).

Experiments involving Fra2 were done with an anti-Fra2 anti-

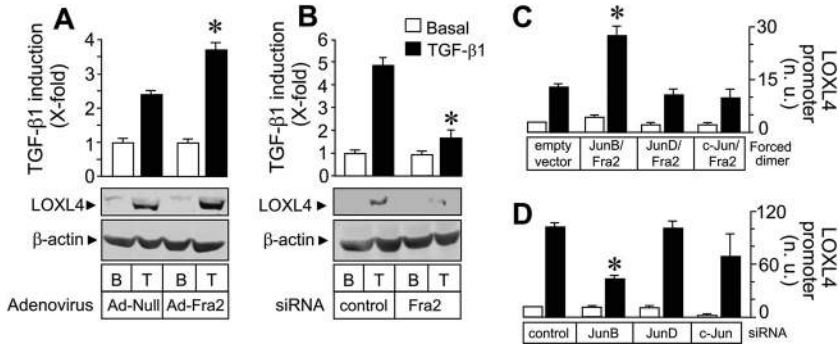

FIG 5 Involvement of Fra2 in the effect of TGF-β1 on LOXL4 expression. (A) Adenovirus-mediated overexpression of Fra2 potentiates the action of TGF-β1 on LOXL4 expression as assessed by luciferase reporter and Western blotting. (B) siRNA-mediated downregulation of Fra2 inhibits TGF-β1-mediated induction of LOXL4 expression. (C) Effect of overexpression of forced AP-1 dimers, including JunB/Fra2, JunD/Fra2, and c-Jun/Fra2, on TGF-β1-induced LOXL4 promoter activity. (D) Effect of siRNA-mediated downregulation of Jun members (JunB, JunD, and c-Jun) on TGF-β1-induced LOXL4 promoter activity. Values are represented either as fold induction with respect to basal values with null adenovirus or siRNA control or as normalized luciferase units (mean ± SEM; $n = 3$), *, $P < 0.05$ versus null adenovirus or empty vector (A and C), or versus siRNA control (B and D), in the presence of TGF-β1. Validation of overexpression or siRNA-mediated downregulation is shown in Fig. S7 in the supplemental material.

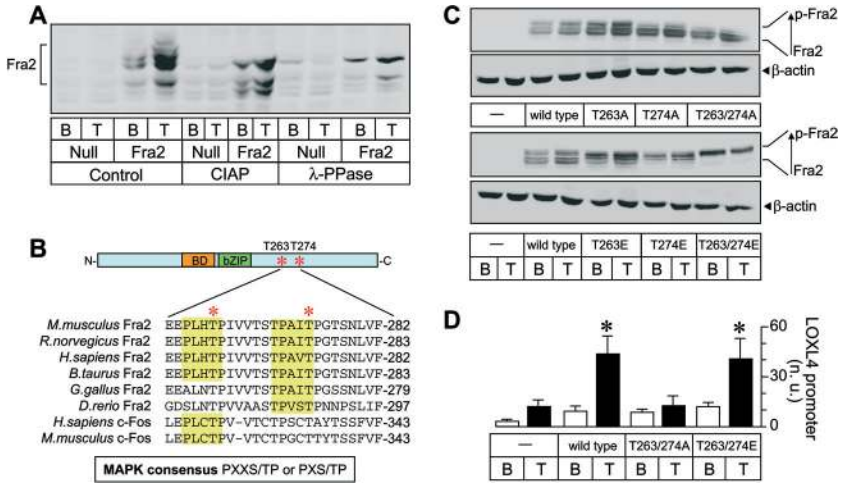

FIG 6 TGF-β1 promotes the phosphorylation of Fra2. (A) Protein extracts from BAEC infected with null or Fra2 adenoviruses and stimulated with TGF-β1 or basal were either left untreated or preincubated with calf intestinal alkaline phosphatase (CIAP) (1 unit/μg protein) or with λ-phosphatase (λ-PPase) (3 units/μg protein) for 1 h, followed by detection of Fra2 by Western blotting. Note that high-MW bands were eliminated with CIAP and λ-PPase, likely corresponding to hyperphosphorylated forms. (B) Domain structure of mouse Fra2 protein. Sequences from several Fra2 and c-Fos orthologs were aligned to show the conserved motifs for MAPK consensus phosphorylation sites (*). Note that the mouse T274-containing motif is conserved among all species compared in this study, whereas T263 is partially conserved in some Fra2 orthologs and in human and mouse c-Fos. (C) Analysis of electrophoretic mobility of Flag-tagged Fra2 with point mutations in MAPK consensus phosphorylation sites T263 and T274. Single and double inactivating T→A or phosphomimetic T→E mutant constructs were transiently transfected into bovine aortic endothelial cells with and without TGF-β1 incubation, and protein extracts were analyzed by Western blotting using an anti-Flag antibody. (D) Luciferase activity of LOXL4 promoter luciferase construct cotransfected with wild-type, T263/274A, and T263/274E Fra2 overexpression plasmids. Values are represented as normalized units for luciferase activity (mean ± SEM; $n = 3$). *, $P < 0.05$ versus pcDNA3 empty vector (−) in the presence of TGF-β1.

body raised against mouse Fra2 protein, which unfortunately did not react with the endogenous Fra2 from bovine aortic endothelial cells but very efficiently recognized the overexpressed mouse isoform. Using this antibody in overexpression experiments, we noticed that the reactivity of Fra2 bands increased significantly upon TGF-β1 stimulation, an observation that was accompanied by the detection of higher-molecular-weight (higher-MW) immunoreactive bands (Fig. 6A; see Fig. S7A in the supplemental material). Immunofluorescence experiments performed with the same protocol showed specific nuclear Fra2 staining that strongly increased after TGF-β1 incubation (see Fig. S7B in the supplemental material). Protein phosphorylation may be compatible with the observed changes in immunoreactivity and MW, and as such it is a posttranslational modification previously reported for Fra2 (38, 39). To demonstrate the potential use of this antibody to reveal phosphorylated Fra2 and therefore the ability of TGF-β1 to induce the phosphorylation of this factor, cell extracts were incubated with calf intestine alkaline phosphatase (CIAP) and λ-phosphatase (λ-PPase), conditions shown to dephosphorylate serine, threonine, and tyrosine residues in proteins (40). As shown also in Fig. 6A, dephosphorylation of cell extracts diminished significantly the increase in immunoreactivity, an effect particularly evident with λ-phosphatase, and, more interestingly, eliminated the higher-MW Fra2 bands, which presumably correspond to heavily phosphorylated forms of the protein. The noncanonical TGF-β signaling pathway has been associated with the activation of members of the mitogen-activated protein kinase (MAPK) family (30). Screening of the sequences of the Fra2 protein among different species, including mouse, rat, human, bovine, chicken, and zebrafish, revealed the presence of two MAPK phosphorylation consensus sites (P-X-X-S/T-P or P-X-S/T-P), in particular, two threonine residues in the C-terminal domain (T263 and T274 in the mouse Fra2), highly conserved in most of Fra2 orthologs and in human and mouse c-Fos proteins (Fig. 6B). Flag-tagged Fra2 constructs with inactivating mutations of threonine to nonphosphorylatable alanine were generated, and the pattern of Flag-tagged Fra2 expression upon TGF-β1 stimulation was analyzed by SDS-PAGE and anti-Flag Western blotting. As shown in Fig. 6C, the T274A substitution resulted in a clear decrease in the detection of high-MW, hyperphosphorylated bands that otherwise were observed with the wild type and the T263A mutant. The construct including both mutations behaved essentially like the T274A mutant. As an alternative approach, glutamic acid substitution mutagenesis, a modification mimicking the structure of a phosphorylated threonine residue, was also introduced. Figure 6C shows that the T274E and, to a lesser extent, T263E substitutions shifted the detected immunoreactive bands into high-MW forms, an effect more clearly evident in the double mutant. These results indicate that phosphorylation of Fra2 in these residues, particularly in the highly conserved T274, may play an important role in the action of TGF-β1. In order to test the ability of the Fra2 mutants to induce TGF-β1-induced LOXL4 expression, we cotransfected wild-type, T263/274A (inactivating), and T263/274E (phosphomimetic) Fra2 plasmids together with the LOXL4 promoter luciferase construct. As shown also in Fig. 6D, the overexpression of wild-type or T263/274E Fra2 strongly potentiated TGF-β1-induced LOXL4 promoter activity, whereas the mutant T263/274A was without any effect. We have also investigated the mechanism(s) by which Fra2 phosphorylation gives rise to a potentiation of LOXL4 expression. First, we analyzed whether the interaction of JunB/Fra2 complex with DNA is affected by Fra2 phosphorylation. *In vitro*-synthesized JunB/Fra2 forced dimers, either wild type, T263/274A, or T263/274E, showed very similar DNA binding activity as assessed by EMSA (see Fig. S8A and B in the sup-

plemental material). We next investigated whether Fra2 phosphorylation facilitates JunB/Fra2 dimerization using GST-Fra2 forms in pulldown experiments. As shown in Fig. S8C in the supplemental material (input), JunB expression was induced upon TGF-β1 stimulation in BAEC, a result that was also observed by microarray analysis (GEO accession number GSE42932). GST-Fra2 beads were incubated with total extracts from BAEC incubated under basal conditions or with TGF-β1 for 24 h, extensively washed, and loaded onto SDS-polyacrylamide gels for Western blot analysis of JunB. GST-Fra2, either wild type, T263/274A, or T263/274E, pulled down endogenous JunB protein with similar capacities. These results indicate that Fra2 phosphorylation does not significantly modify DNA binding activity or dimer formation of AP-1 complexes.

TGF-β1-dependent Fra2 phosphorylation likely involves the activation of a MAPK. We next analyzed the effects of specific pharmacological inhibitors of p38, ERK, and JNK MAPKs on the upregulation of LOXL4 promoter activity by TGF-β1. As shown in Fig. 7A, the blockade of the ERK pathway strongly attenuated the action of TGF-β1, whereas the inhibitors of p38 and JNK did not show any significant effect. Dose-dependent analysis of the effect of the ERK inhibitor, CI-1040, showed that this compound diminished TGF-β1-induced LOXL4 mRNA and promoter activity at concentrations reported to specifically inhibit ERK phosphorylation (100 to 500 nM) (Fig. 7B and C) (41). We also studied the time course of the effect of TGF-β1 on ERK and Fra2 phosphorylation by Western blotting. TGF-β1 very rapidly induced an increase in the phosphorylation status of ERK, which was followed by the detection of hyperphosphorylated forms of Fra2 (Fig. 7D). Both actions of TGF-β1 were strongly abolished by preincubation of the ERK inhibitor. These results indicate that TGF-β1 induction of LOXL4 expression requires the activation of the ERK pathway and subsequent ERK-dependent phosphorylation of Fra2.

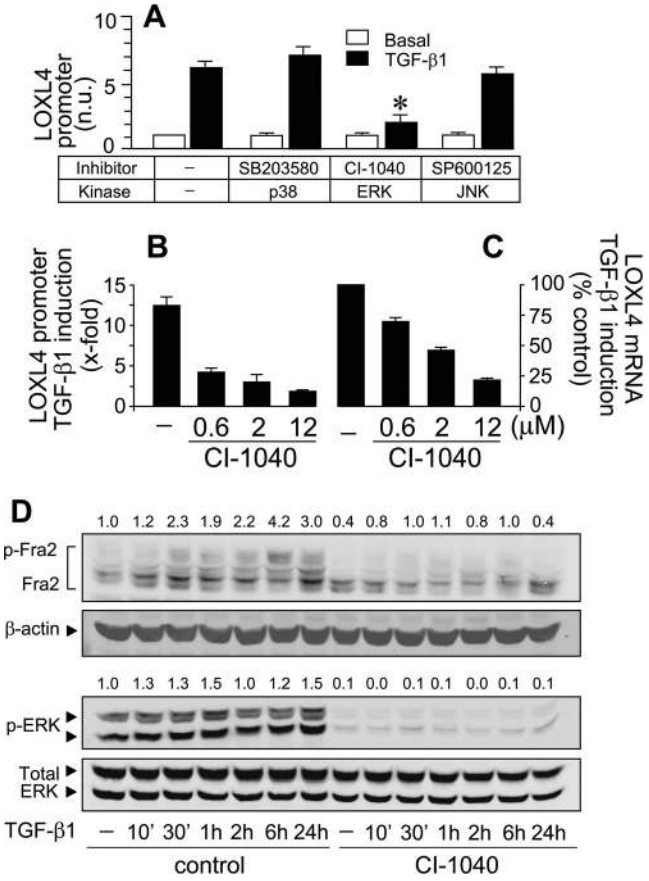

FIG 7 TGF-β1 induces LOXL4 expression by ERK-mediated phosphorylation of Fra2. (A) Effects of MAPK inhibitors SB203580 (p38, 10 μM), CI-1040 (ERK, 2 μM), and SP600125 (JNK, 25 μM) on luciferase activity of LOXL4 promoter luciferase construct. Values are represented as normalized luciferase units (mean ± SEM; $n = 3$). *, $P < 0.05$ versus vehicle (dimethyl sulfoxide [DMSO] for SB203580 and CI-1040 and ethanol for SP600125) upon TGF-β1 stimulation. (B and C) Dose dependence analysis of the effect of the ERK inhibitor CI-1040 on TGF-β1-induced LOXL4 promoter activity (B) and mRNA expression (C). (D) Time course of the effect of TGF-β1 on ERK activation (phospho-ERK [p-ERK]) and Fra2 phosphorylation (p-Fra2) analyzed by Western blotting in extracts from cells treated with vehicle (control) or with CI-1040 (2 μM). Values above the blots refer to the p-Fra2/β-actin and p-ERK/total ERK ratios after densitometric analysis. Results are representative of three experiments.

LOXL4 contributes to the matrix remodeling action of TGF-β1 in aortic endothelial cells. LOXL4 is the most recently identified member of the lysyl oxidase family. Therefore, little information is available on LOXL4 subcellular localization and function, particularly in the cardiovascular system (42–44). The C-terminal region of LOXL4 protein contains a catalytic domain highly homologous to other lysyl oxidases. On the other hand, the N-terminal region has four scavenger receptor cysteine-rich (SRCR) domains that are conserved only in the LOXL2 and LOXL3 isoforms. To gain insight into the subcellular localization of LOXL4 protein and to individually analyze the contributions of its different domains, we generated a LOXL4-GFP fusion protein and deletion mutants thereof lacking the SRCR domains and the C-terminal catalytic region (Fig. 8A). Cell transfection with the full-length LOXL4-GFP construct showed that the fluorescent signal was perinuclear, spatially overlapping with the immunocytochemical detection of calnexin, a typical endoplasmic reticulum (ER) marker (Fig. 8B). This subcellular distribution is roughly maintained upon removal of the SRCR domains, but it is heavily affected by deletion of the C-terminal catalytic region, whose fluorescence was homogeneously diffuse throughout the cell, much in the same way as GFP only (see Fig. S9 in the supplemental material). The localization of the full-length protein in the ER compartment suggests that LOXL4 may transit through the ER as a part of the secretory pathway, yielding its release into the extracellular medium. To evaluate this hypothesis, we generated stable transfectants of human embryonic kidney 293 (HEK 293) cells expressing the aforementioned set of LOXL4-GFP constructs. Analysis by anti-GFP Western blotting showed that these isogenic clones of HEK 293 cells expressed the corresponding LOXL4-GFP proteins (Fig. 8C, Cells). The extracellular medium accumulated for 48 h was concentrated and analyzed by Western blotting. As shown also in Fig. 8C (Media), full-length LOXL4-GFP was clearly detectable in the extracellular medium, indicating that this protein is indeed extracellularly secreted. The presence of multiples copies of the SCRC domains seems to be essential for the extracellular release, as elimination of more than one of these repeats impaired the accumulation of the protein in the extracellular medium. LOXL4-GFP ΔC-t, a deletion construct with intact SRCR domains, was again recovered from the extracellular medium. Similar experiments performed with BAEC incubated with TGF-β1 or infected with a LOXL4-overexpressing adenovirus also

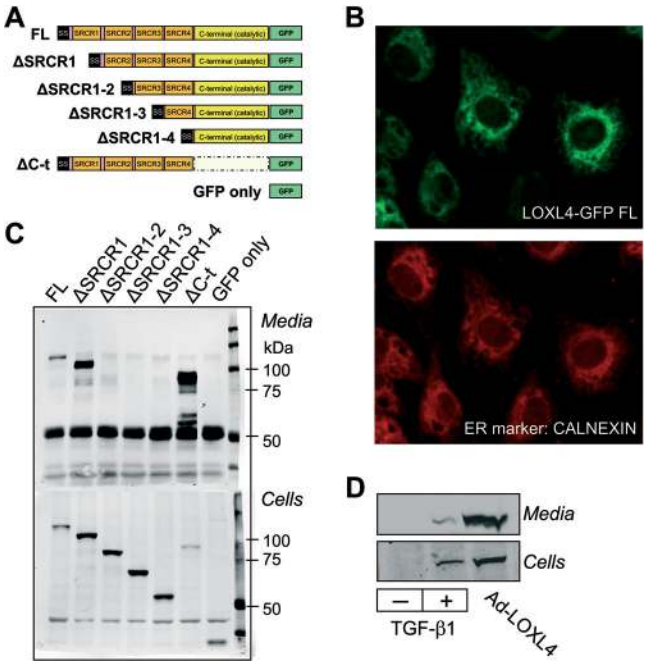

FIG 8 Subcellular localization and extracellular secretion of LOXL4 in aortic endothelial cells. (A) Domain structure of full-length (FL) LOXL4-GFP fusion protein and deletion mutants thereof lacking the SRCR domains and the C-terminal catalytic region. (B) Subcellular localization of full-length LOXL4-GFP expressed in bovine aortic endothelial cells by adenoviral infection as assessed by GFP fluorescence microscopy (upper panel) and colocalization of the endoplasmic reticulum marker calnexin by immunofluorescence (lower panel). (C) Analysis of the extracellular secretion of LOXL4-GFP chimeras stably expressed in HEK 293 cells by Western blotting using anti-GFP antibody. Note the presence of secreted GFP-immunoreactive bands in FL, ΔSRCR1, and ΔC-t. (D) Extracellular secretion of endogenous LOXL4 upon TGF-β1 incubation in aortic endothelial cells as assessed by Western blotting with anti-LOXL4 antibody. The secretion of LOXL4-GFP from cells infected with the corresponding adenovirus is also shown (Media, supernatant; Cells, cell extract). Results are representative of three experiments.

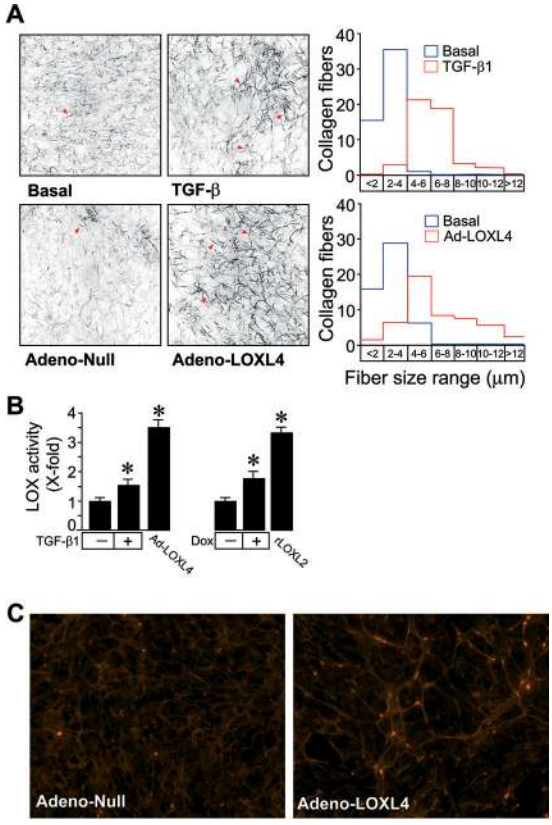

FIG 9 LOXL4 expression leads to matrix remodeling. (A) Type I collagen solution was mixed with medium from cells left under basal conditions, exposed to TGF-β1, or infected with LOXL4 or null adenoviruses, and fibrillar collagen formation was monitored by confocal reflection microscopy. Collagen fiber number and size were counted in at least three random fields and represented as number of fibers per range of size. (B) Lysyl oxidase activity as assessed by H_2O_2 Amplex determination in supernatants from BAEC with or without TGF-β1 stimulation or infected with Ad-LOXL4 and in HEK 293 cells treated with or without doxycycline (Dox). A positive control with recombinant human LOXL2 is also shown. (C) Increased collagen IV deposition and assembly by BAEC infected with adeno-LOXL4 compared with adeno-null visualized by immunofluorescence microscopy. Results are representative of at least three experiments.

showed the presence of extracellularly secreted LOXL4 protein (Fig. 8D).

To explore the contribution of LOXL4 to collagen cross-linking, we incubated soluble type I collagen with conditioned medium generated by aortic endothelial cells incubated for 48 h in the presence or absence of TGF-β1 and with empty vector or LOXL4-overexpressing adenoviruses, and fibrillar collagen was imaged by confocal reflection microscopy. As shown in Fig. 9A, based on fiber size, fibrillar collagen formation was strongly enhanced in samples incubated with medium from cells exposed to TGF-β1 or infected with LOXL4 adenovirus. This matrix-remodeling capacity was consistent with the classical determination of lysyl oxidase activity by detection of H_2O_2 using Amplex red as assessed in both endothelial cells and HEK 293 cells overexpressing LOXL4 (Fig. 9B). The ability of LOXL4 to regulate the deposition and assembly of collagen IV was analyzed by immunofluorescence microscopy. As shown in Fig. 9C, cells overexpressing LOXL4 showed increased collagen IV network assembly compared to control cells. These data suggest that LOXL4 may play a role in collagen IV assembly in the subendothelial basement membrane, therefore contributing significantly to vascular extracellular microenvironment.

DISCUSSION

The role of LOX enzymes in human pathophysiology has attracted considerable interest in recent years, as elevated expression and/or activity has been associated with several diseases, particularly of the vascular system, and with tumorigenesis (45, 46). As long as biological mechanisms for the control of LOX activity remain unknown, the main point of regulation is the control of the expression of LOX family members. TGF-β1 has revealed as an important factor for the regulation of the expression of LOX isoforms in different cells and tissues (47–49). LOXL4 has also been recently described to be upregulated by TGF-β signaling in hepatoma cells, though the exact molecular mechanism for this action was not studied in depth (26). The present work describes in detail, to our knowledge for the first time, the regulation of the expression of LOXL4 by TGF-β1 in bovine aortic endothelial cells. According to our results, transcriptional activation of the LOXL4 promoter accounted for the TGF-β1-induced increase in LOXL4 expression. We have identified a genomic region at about 4 kb upstream of the transcription initiation site that is responsible for the effect of

TGF-β1. This genomic fragment, which behaves as a sensitive TGF-β1-activated enhancer, contains specific binding sites for AP-1 and Smad transcription factors. Specific mutation of these elements abolished TGF-β1 responsiveness, as well as the binding activity of these factors. The cooperation between Smad and AP-1 transcription factors is essential to determine TGF-β signaling to the nucleus, and examples from the literature include the genes encoding endothelin 1 (ET-1), follicle-stimulating hormone β (FSHB), and tumor necrosis factor-related apoptosis-inducing ligand (TRAIL), among others (12, 50, 51). In fact, AP-1 sites have been shown to be the most enriched motif in Smad2/3 regions identified recently in a ChIP-on-chip analysis (52). Interestingly, this report successfully identified the enhancer within the LOXL4 promoter characterized here as a Smad2/3 binding region in HaCaT cells, and it proposed LOXL4 as a TGF-β-inducible gene. Comparative sequence analysis of 5′ flanking regions of mammalian LOXL4 orthologs showed that this region indeed is evolutionarily well conserved, with the AP-1 site and the Smad binding elements present in most mammalian genomes. Surprisingly, the AP-1 site was not conserved in rodent orthologs, and this observation is consistent with the lack of response to TGF-β1 by the mouse LOXL4 gene. These results indicate that selective constraints acting on this region may have been relaxed in the mouse and rat species, as is estimated to have occurred with 30 to 40% of the human functional sites, an aspect raising concerns about the generalization of the regulation of expression and likely also of the function of LOXL4 in the rodent models (53).

The present work identified Fra2 as the AP-1 component interacting with the AP-1 site within the LOXL4 promoter and contributing to the action of TGF-β1 on LOXL4 expression. This finding further supports the notion that Fra2 may act as a novel downstream mediator of the effect of TGF-β1 on matrix remodeling and fibrosis. Strong expression of Fra2 was detected in lung samples from patients with idiopathic pulmonary fibrosis (33). Additionally, Fra2 was found to be overexpressed in the dermis of patients with scleroderma, where it has been proposed to play a role in the induction of ECM proteins upon TGF-β1 stimulation (34, 36). Transgenic mice overexpressing Fra2 develop extensive fibrosis in several organs, with the pulmonary tissue being particularly affected, which is initiated as a severe vasculopathy characterized by vascular remodeling and obliteration of pulmonary arteries (35). Based on these observations and our own results in vascular endothelial cells, it can be hypothesized that Fra2 mediates a specific TGF-β1-dependent, ECM-specific genetic program in the vasculature, which can eventually contribute to the development of fibrosis. Experiments in dermal fibroblasts from scleroderma patients have also shown that the inhibition of the ERK pathway impairs Fra2-dependent collagen production (36). In fact, ERK has been largely implicated in the activation of fibrotic responses, both in the skin and in the cardiovascular system, and in agreement with our results, this kinase is phosphorylated and activated upon stimulation with TGF-β1 (54–56). We also report here that TGF-β1 promotes the ERK-dependent phosphorylation of Fra2 and, based on mutagenesis experiments, identified T274 and (to a lesser extent) T263 as the phosphorylation sites of mouse Fra2 required to promote TGF-β1-dependent LOXL4 expression. The mechanism by which Fra2 phosphorylation regulates gene transcription seems not to involve increased DNA binding or AP-1 complex formation.

Fra2 requires dimerization with a Jun partner in order to form the AP-1 complex capable of binding DNA, and according to our results, this role is supported by JunB. Recent reports have delineated the essential role of JunB in TGF-β-induced fibrotic responses (57). In fact, JunB not only contributes to matrix production and deposition but is an integral part of the TGF-β-induced epithelial-to-mesenchymal transition (EMT) process. Today it has become clear that endothelial cells can also transition into mesenchymal cells and that TGF-β1 is a primary inducer of this process (58, 59). The extent of this transdifferentiation correlates with the acquisition of smooth muscle cell (SMC) markers, potentially serving this process as a source of smooth muscle cells in vascular neointimal lesions (60, 61). Under our experimental conditions, TGF-β1 stimulation of bovine aortic endothelial cells did not promote the expression of α-smooth muscle actin (α-SMA), the *bona fide* marker of SMC differentiation, but we did observe the induction of other SMC-specific genes, for example, those for cysteine and glycine-rich protein 2 (CSRP2), transgrelin (SM22α), and ankyrin repeat domain 1 (ANKRD1) (see microarray data) (62–64). It is tempting to speculate whether LOXL4 may also be assigned to the category of SMC genes contributing to proliferation, migration, and matrix deposition and associated with the development of intimal thickening and other vascular pathologies.

TGF-β1 activation of the endothelium, both under cell culture conditions and in the native endothelium, has been also shown to induce the formation of podosomes, which are specialized plasma membrane actin-based microdomains endowed, in a manner similar to that for invadopodia, with adhesive and matrix-degrading activities (65, 66). Degradation of the underlying basement membrane by podosome-localized proteases is associated with vessel ECM remodeling and tissue invasion. It can be hypothesized that basement membrane proteolysis by podosomes and further LOXL4-based matrix cross-linking constitute early (degradative) and late (reparative) responses of the endothelium to TGF-β1 stimulation, respectively. Type IV collagen polymers, the predominant scaffolding of basement membranes, are stabilized by a network of covalent cross-links (67). Unlike fibrillar collagens (types I, II, III, V, and XI), where LOX-mediated cross-linking has been largely demonstrated to occur, the implication of LOX family members in the assembly of type IV collagen networks is still an open question (68). The present work for LOXL4 and our recent report for LOXL2 showed that these enzymes contribute significantly to type IV collagen deposition in the ECM (69). These findings indicate an active role for these enzymes in the assembly of type IV collagen networks, further supporting the long-appreciated observation that this type of collagen cannot be efficiently extracted from basement membranes assembled *in vivo* unless the animals are fed a lathyrogen (i.e., a compound such as β-aminopropionitrile that inhibits LOX activity, therefore preventing collagen cross-linking) (70).

Early reports on the biochemical properties of LOXL4 described this protein as an extracellularly secreted factor (44). We confirmed here this observation and further analyzed the role of the SRCR domains in the release of the protein. Our results showed unequivocally that SRCR domains are required for LOXL4 to be detected in the extracellular medium. SRCR domains constitute ancient and highly conserved protein modules present in a number of soluble or membrane-bound proteins for which no unifying function has been so far defined (71). A recent report has shown that the enzymatic activity of LOXL2 is not

altered upon deletion of SRCR domains (72). This observation and our own results suggest that N-terminal SRCR-containing domains and C-terminal catalytic region provide LOXL isoforms with independent capabilities, with the former likely contributing to protein secretion and the latter being responsible for the enzymatic activity.

In summary, we describe here the identification of the LOXL4 gene as a TGF-β1 target gene in bovine aortic endothelial cells and the characterization of the molecular mechanism utilized by this cytokine to induce the expression of the LOXL4 gene. We show that TGF-β1 activates both canonical (Smad-dependent) and noncanonical (Smad-independent, ERK-dependent) signaling pathways, which require AP-1 and Smad sites identified within an upstream TGF-β1-activated enhancer in the LOXL4 promoter. We also provide evidence that LOXL4 is extracellularly secreted and significantly contributes *in vitro* to ECM deposition. Based on our results, we propose that TGF-β1-dependent expression of LOXL4 might have pathophysiological implications in vascular processes associated with matrix remodeling and fibrosis.

ACKNOWLEDGMENTS

This work was supported by grants from the Ministerio de Economía y Competitividad (Plan Nacional de I+D+I: SAF2009-09085, SAF2012-34916), Comunidad Autónoma de Madrid (2010-BMD2321, FIBROTEAM Consortium), Fundación Genoma España (MEICA project), Consejo Superior de Investigaciones Científicas (Proyecto Intramural de Incorporación, 200920I158), and Fundación Renal Iñigo Alvárez de Toledo. O.B. is a recipient of a fellowship from the Ministerio de Economía y Competitividad (Formación de Personal Investigador).

We thank Santiago Lamas (Madrid, Spain) for helpful discussion, comments, and continuous support. We thank Macarena Quesada, Eva M. Blanco, and Jorge García for their technical assistance.

REFERENCES

1. **Wu MY, Hill CS.** 2009. Tgf-beta superfamily signaling in embryonic development and homeostasis. Dev. Cell **16**:329–343.
2. **Attisano L, Wrana JL.** 2002. Signal transduction by the TGF-beta superfamily. Science **296**:1646–1647.
3. **Leask A, Abraham DJ.** 2004. TGF-beta signaling and the fibrotic response. FASEB J. **18**:816–827.
4. **Ruiz-Ortega M, Rodriguez-Vita J, Sanchez-Lopez E, Carvajal G, Egido J.** 2007. TGF-beta signaling in vascular fibrosis. Cardiovasc. Res. **74**:196–206.
5. **Graham HK, Akhtar R, Kridiotis C, Derby B, Kundu T, Trafford AW, Sherratt MJ.** 2011. Localised micro-mechanical stiffening in the ageing aorta. Mech. Ageing Dev. **132**:459–467.
6. **Pick R, Jalil JE, Janicki JS, Weber KT.** 1989. The fibrillar nature and structure of isoproterenol-induced myocardial fibrosis in the rat. Am. J. Pathol. **134**:365–371.
7. **Lindeman JH, Ashcroft BA, Beenakker JW, van Es M, Koekkoek NB, Prins FA, Tielemans JF, Abdul-Hussien H, Bank RA, Oosterkamp TH.** 2010. Distinct defects in collagen microarchitecture underlie vessel-wall failure in advanced abdominal aneurysms and aneurysms in Marfan syndrome. Proc. Natl. Acad. Sci. U. S. A. **107**:862–865.
8. **Birk DE, Bruckner P.** 2011. Collagens, suprastructures, and collagen fibril assembly, p 1–39. *In* Mecham RP (ed), The extracellular matrix: an overview. Springer-Verlag, Berlin, Germany.
9. **Maki JM.** 2009. Lysyl oxidases in mammalian development and certain pathological conditions. Histol. Histopathol. **24**:651–660.
10. **Liu X, Zhao Y, Gao J, Pawlyk B, Starcher B, Spencer JA, Yanagisawa H, Zuo J, Li T.** 2004. Elastic fiber homeostasis requires lysyl oxidase-like 1 protein. Nat. Genet. **36**:178–182.
11. **Maki JM, Rasanen J, Tikkanen H, Sormunen R, Makikallio K, Kivirikko KI, Soininen R.** 2002. Inactivation of the lysyl oxidase gene Lox leads to aortic aneurysms, cardiovascular dysfunction, and perinatal death in mice. Circulation **106**:2503–2509.
12. **Rodriguez-Pascual F, Redondo-Horcajo M, Lamas S.** 2003. Functional cooperation between Smad proteins and activator protein-1 regulates transforming growth factor-beta-mediated induction of endothelin-1 expression. Circ. Res. **92**:1288–1295.
13. **Piek E, Ju WJ, Heyer J, Escalante-Alcalde D, Stewart CL, Weinstein M, Deng C, Kucherlapati R, Bottinger EP, Roberts AB.** 2001. Functional characterization of transforming growth factor beta signaling in Smad2- and Smad3-deficient fibroblasts. J. Biol. Chem. **276**:19945–19953.
14. **Rodriguez-Pascual F, Redondo-Horcajo M, Magan-Marchal N, Lagares D, Martinez-Ruiz A, Kleinert H, Lamas S.** 2008. Glyceraldehyde-3-phosphate dehydrogenase regulates endothelin-1 expression by a novel, redox-sensitive mechanism involving mRNA stability. Mol. Cell. Biol. **28**:7139–7155.
15. **Chomczynski P, Sacchi N.** 1987. Single-step method of RNA isolation by acid guanidinium thiocyanate-phenol-chloroform extraction. Anal. Biochem. **162**:156–159.
16. **Livak KJ, Schmittgen TD.** 2001. Analysis of relative gene expression data using real-time quantitative PCR and the 2(−Delta Delta C(T)) method. Methods **25**:402–408.
17. **Matsuo K, Owens JM, Tonko M, Elliott C, Chambers TJ, Wagner EF.** 2000. Fosl1 is a transcriptional target of c-Fos during osteoclast differentiation. Nat. Genet. **24**:184–187.
18. **Bakiri L, Matsuo K, Wisniewska M, Wagner EF, Yaniv M.** 2002. Promoter specificity and biological activity of tethered AP-1 dimers. Mol. Cell. Biol. **22**:4952–4964.
19. **Ovcharenko I, Loots GG, Giardine BM, Hou M, Ma J, Hardison RC, Stubbs L, Miller W.** 2005. Mulan: multiple-sequence local alignment and visualization for studying function and evolution. Genome Res. **15**:184–194.
20. **Schreiber E, Matthias P, Muller MM, Schaffner W.** 1989. Rapid detection of octamer binding proteins with 'mini-extracts', prepared from a small number of cells. Nucleic Acids Res. **17**:6419.
21. **Shevchenko A, Wilm M, Vorm O, Mann M.** 1996. Mass spectrometric sequencing of proteins from silver-stained polyacrylamide gels. Anal. Chem. **68**:850–858.
22. **Lagares D, Busnadiego O, Garcia-Fernandez RA, Kapoor M, Liu S, Carter DE, Abraham DJ, Shi-Wen X, Carreira P, Fontaine BA, Shea BS, Tager AM, Leask A, Lamas S, Rodriguez-Pascual F.** 2012. Inhibition of focal adhesion kinase prevents experimental lung fibrosis and myofibroblast formation. Arthritis Rheum. **64**:1653–1664.
23. **Artym VV, Matsumoto K.** 2010. Imaging cells in three-dimensional collagen matrix. Curr. Protoc. Cell Biol. **Chapter 10**:Unit 10.18.1–10.18.20.
24. **Palamakumbura AH, Trackman PC.** 2002. A fluorometric assay for detection of lysyl oxidase enzyme activity in biological samples. Anal. Biochem. **300**:245–251.
25. **Gorogh T, Holtmeier C, Weise JB, Hoffmann M, Ambrosch P, Laudien M, Csiszar K.** 2008. Functional analysis of the 5′ flanking domain of the LOXL4 gene in head and neck squamous cell carcinoma cells. Int. J. Oncol. **33**:1091–1098.
26. **Kim DJ, Lee DC, Yang SJ, Lee JJ, Bae EM, Kim DM, Min SH, Kim SJ, Kang DC, Sang BC, Myung PK, Park KC, Yeom YI.** 2008. Lysyl oxidase like 4, a novel target gene of TGF-beta1 signaling, can negatively regulate TGF-beta1-induced cell motility in PLC/PRF/5 hepatoma cells. Biochem. Biophys. Res. Commun. **373**:521–527.
27. **Sundqvist A, Zieba A, Vasilaki E, Herrera Hidalgo C, Soderberg O, Koinuma D, Miyazono K, Heldin CH, Landegren U, Ten Dijke P, van Dam H.** 27 August 2012. Specific interactions between Smad proteins and AP-1 components determine TGFbeta-induced breast cancer cell invasion. Oncogene doi:10.1038/onc.2012.370.
28. **Chung K-Y, Agarwal A, Uitto J, Mauviel A.** 1996. An AP-1 binding sequence is essential for regulation of the human 2(I) collagen (COL1A2) promoter activity by transforming growth factor. J. Biol. Chem. **271**:3272–3278.
29. **Macleod D, Charlton J, Mullins J, Bird AP.** 1994. Sp1 sites in the mouse aprt gene promoter are required to prevent methylation of the CpG island. Genes Dev. **8**:2282–2292.
30. **Derynck R, Zhang YE.** 2003. Smad-dependent and Smad-independent pathways in TGF-beta family signalling. Nature **425**:577–584.
31. **Matthews CP, Birkholz AM, Baker AR, Perella CM, Beck GR Jr, Young MR, Colburn NH.** 2007. Dominant-negative activator protein 1 (TAM67) targets cyclooxygenase-2 and osteopontin under conditions in which it specifically inhibits tumorigenesis. Cancer Res. **67**:2430–2438.

32. **Moustakas A, Heldin CH.** 2009. The regulation of TGFbeta signal transduction. Development **136**:3699–3714.
33. **Eferl R, Hasselblatt P, Rath M, Popper H, Zenz R, Komnenovic V, Idarraga MH, Kenner L, Wagner EF.** 2008. Development of pulmonary fibrosis through a pathway involving the transcription factor Fra-2/AP-1. Proc. Natl. Acad. Sci. U. S. A. **105**:10525–10530.
34. **Maurer B, Busch N, Jungel A, Pileckyte M, Gay RE, Michel BA, Schett G, Gay S, Distler J, Distler O.** 2009. Transcription factor fos-related antigen-2 induces progressive peripheral vasculopathy in mice closely resembling human systemic sclerosis. Circulation **120**:2367–2376.
35. **Maurer B, Reich N, Juengel A, Kriegsmann J, Gay RE, Schett G, Michel BA, Gay S, Distler JH, Distler O.** 2012. Fra-2 transgenic mice as a novel model of pulmonary hypertension associated with systemic sclerosis. Ann. Rheum. Dis. **71**:1382–1387.
36. **Reich N, Maurer B, Akhmetshina A, Venalis P, Dees C, Zerr P, Palumbo K, Zwerina J, Nevskaya T, Gay S, Distler O, Schett G, Distler JH.** 2010. The transcription factor Fra-2 regulates the production of extracellular matrix in systemic sclerosis. Arthritis Rheum. **62**:280–290.
37. **O'Shea EK, Rutkowski R, Kim PS.** 1992. Mechanism of specificity in the Fos-Jun oncoprotein heterodimer. Cell **68**:699–708.
38. **Murakami M, Sonobe MH, Ui M, Kabuyama Y, Watanabe H, Wada T, Handa H, Iba H.** 1997. Phosphorylation and high level expression of Fra-2 in v-src transformed cells: a pathway of activation of endogenous AP-1. Oncogene **14**:2435–2444.
39. **Murakami M, Ui M, Iba H.** 1999. Fra-2-positive autoregulatory loop triggered by mitogen-activated protein kinase (MAPK) and Fra-2 phosphorylation sites by MAPK. Cell Growth Differ. **10**:333–342.
40. **Husberg C, Agnetti G, Holewinski RJ, Christensen G, Van Eyk JE.** 2012. Dephosphorylation of cardiac proteins in vitro—a matter of phosphatase specificity. Proteomics **12**:973–978.
41. **Sebolt-Leopold JS, Dudley DT, Herrera R, Van Becelaere K, Wiland A, Gowan RC, Tecle H, Barrett SD, Bridges A, Przybranowski S, Leopold WR, Saltiel AR.** 1999. Blockade of the MAP kinase pathway suppresses growth of colon tumors in vivo. Nat. Med. **5**:810–816.
42. **Asuncion L, Fogelgren B, Fong KS, Fong SF, Kim Y, Csiszar K.** 2001. A novel human lysyl oxidase-like gene (LOXL4) on chromosome 10q24 has an altered scavenger receptor cysteine rich domain. Matrix Biol. **20**:487–491.
43. **Ito H, Akiyama H, Iguchi H, Iyama K, Miyamoto M, Ohsawa K, Nakamura T.** 2001. Molecular cloning and biological activity of a novel lysyl oxidase-related gene expressed in cartilage. J. Biol. Chem. **276**:24023–24029.
44. **Maki JM, Tikkanen H, Kivirikko KI.** 2001. Cloning and characterization of a fifth human lysyl oxidase isoenzyme: the third member of the lysyl oxidase-related subfamily with four scavenger receptor cysteine-rich domains. Matrix Biol. **20**:493–496.
45. **Barker HE, Cox TR, Erler JT.** 2012. The rationale for targeting the LOX family in cancer. Nat. Rev. Cancer **12**:540–552.
46. **Lopez B, Gonzalez A, Hermida N, Valencia F, de Teresa E, Diez J.** 2010. Role of lysyl oxidase in myocardial fibrosis: from basic science to clinical aspects. Am. J. Physiol. Heart Circ. Physiol. **299**:H1–H9.
47. **Gacheru SN, Thomas KM, Murray SA, Csiszar K, Smith-Mungo LI, Kagan HM.** 1997. Transcriptional and post-transcriptional control of lysyl oxidase expression in vascular smooth muscle cells: effects of TGF-Î²1 and serum deprivation. J. Cell. Biochem. **65**:395–407.
48. **Boak AM, Roy R, Berk J, Taylor L, Polgar P, Goldstein RH, Kagan HM.** 1994. Regulation of lysyl oxidase expression in lung fibroblasts by transforming growth factor-beta 1 and prostaglandin E2. Am. J. Respir. Cell Mol. Biol. **11**:751–755.
49. **Sethi A, Mao W, Wordinger RJ, Clark AF.** 2011. Transforming growth factor-beta induces extracellular matrix protein cross-linking lysyl oxidase (LOX) genes in human trabecular meshwork cells. Invest. Ophthalmol. Vis. Sci. **52**:5240–5250.
50. **Wang Y, Fortin Jrm, Lamba P, Bonomi M, Persani L, Roberson MS, Bernard DJ.** 2008. Activator protein-1 and Smad proteins synergistically regulate human follicle-stimulating hormone Î²-promoter activity. Endocrinology **149**:5577–5591.
51. **Herzer K, Grosse-Wilde A, Krammer PH, Galle PR, Kanzler S.** 2008. Transforming growth factor-beta-mediated tumor necrosis factor-related apoptosis-inducing ligand expression and apoptosis in hepatoma cells requires functional cooperation between Smad proteins and activator protein-1. Mol. Cancer Res. **6**:1169–1177.
52. **Koinuma D, Tsutsumi S, Kamimura N, Taniguchi H, Miyazawa K, Sunamura M, Imamura T, Miyazono K, Aburatani H.** 2009. Chromatin immunoprecipitation on microarray analysis of Smad2/3 binding sites reveals roles of ETS1 and TFAP2A in transforming growth factor beta signaling. Mol. Cell. Biol. **29**:172–186.
53. **Dermitzakis ET, Clark AG.** 2002. Evolution of transcription factor binding sites in mammalian gene regulatory regions: conservation and turnover. Mol. Biol. Evol. **19**:1114–1121.
54. **Stratton R, Rajkumar V, Ponticos M, Nichols B, Shiwen X, Black CM, Abraham DJ, Leask A.** 2002. Prostacyclin derivatives prevent the fibrotic response to TGF-beta by inhibiting the Ras/MEK/ERK pathway. FASEB J. **16**:1949–1951.
55. **de Boer RA, Pokharel S, Flesch M, van Kampen DA, Suurmeijer AJ, Boomsma F, van Gilst WH, van Veldhuisen DJ, Pinto YM.** 2004. Extracellular signal regulated kinase and SMAD signaling both mediate the angiotensin II driven progression towards overt heart failure in homozygous TGR(mRen2)27. J. Mol. Med. (Berl.) **82**:678–687.
56. **Nakerakanti S, Trojanowska M.** 2012. The role of TGF-beta receptors in fibrosis. Open Rheumatol. J. **6**:156–162.
57. **Gervasi M, Bianchi-Smiraglia A, Cummings M, Zheng Q, Wang D, Liu S, Bakin AV.** 2012. JunB contributes to Id2 repression and the epithelial-to-mesenchymal transition in response to transforming growth factor-beta. J. Cell Biol. **196**:589–603.
58. **Zeisberg EM, Tarnavski O, Zeisberg M, Dorfman AL, McMullen JR, Gustafsson E, Chandraker A, Yuan X, Pu WT, Roberts AB, Neilson EG, Sayegh MH, Izumo S, Kalluri R.** 2007. Endothelial-to-mesenchymal transition contributes to cardiac fibrosis. Nat. Med. **13**:952–961.
59. **Piera-Velazquez S, Li Z, Jimenez SA.** 2011. Role of endothelial-mesenchymal transition (EndoMT) in the pathogenesis of fibrotic disorders. Am. J. Pathol. **179**:1074–1080.
60. **Arciniegas E, Sutton AB, Allen TD, Schor AM.** 1992. Transforming growth factor beta 1 promotes the differentiation of endothelial cells into smooth muscle-like cells in vitro. J. Cell Sci. **103**:521–529.
61. **Arciniegas E, Frid MG, Douglas IS, Stenmark KR.** 2007. Perspectives on endothelial-to-mesenchymal transition: potential contribution to vascular remodeling in chronic pulmonary hypertension. Am. J. Physiol. Lung Cell. Mol. Physiol. **293**:L1–L8.
62. **Frid MG, Kale VA, Stenmark KR.** 2002. Mature vascular endothelium can give rise to smooth muscle cells via endothelial-mesenchymal transdifferentiation: in vitro analysis. Circ. Res. **90**:1189–1196.
63. **Ishisaki A, Hayashi H, Li AJ, Imamura T.** 2003. Human umbilical vein endothelium-derived cells retain potential to differentiate into smooth muscle-like cells. J. Biol. Chem. **278**:1303–1309.
64. **Spin JM, Nallamshetty S, Tabibiazar R, Ashley EA, King JY, Chen M, Tsao PS, Quertermous T.** 2004. Transcriptional profiling of in vitro smooth muscle cell differentiation identifies specific patterns of gene and pathway activation. Physiol. Genomics **19**:292–302.
65. **Varon C, Tatin F, Moreau V, Van Obberghen-Schilling E, Fernandez-Sauze S, Reuzeau E, Kramer I, Genot E.** 2006. Transforming growth factor beta induces rosettes of podosomes in primary aortic endothelial cells. Mol. Cell. Biol. **26**:3582–3594.
66. **Rottiers P, Saltel F, Daubon T, Chaigne-Delalande B, Tridon V, Billottet C, Reuzeau E, Genot E.** 2009. TGFbeta-induced endothelial podosomes mediate basement membrane collagen degradation in arterial vessels. J. Cell Sci. **122**:4311–4318.
67. **Khoshnoodi J, Pedchenko V, Hudson BG.** 2008. Mammalian collagen IV. Microsc. Res. Tech. **71**:357–370.
68. **Eyre DR, Wu JJ.** 2010. Collagen crosslinks. Top. Curr. Chem. **247**:207–229.
69. **Bignon M, Pichol-Thievend C, Hardouin J, Malbouyres M, Brechot N, Nasciutti L, Barret A, Teillon J, Guillon E, Etienne E, Caron M, Joubert-Caron R, Monnot C, Ruggiero F, Muller L, Germain S.** 2011. Lysyl oxidase-like protein-2 regulates sprouting angiogenesis and type IV collagen assembly in the endothelial basement membrane. Blood **118**:3979–3989.
70. **Kleinman HK, McGarvey ML, Liotta LA, Robey PG, Tryggvason K, Martin GR.** 1982. Isolation and characterization of type IV procollagen, laminin, and heparan sulfate proteoglycan from the EHS sarcoma. Biochemistry **21**:6188–6193.
71. **Sarrias MR, Gronlund J, Padilla O, Madsen J, Holmskov U, Lozano F.** 2004. The scavenger receptor cysteine-rich (SRCR) domain: an ancient and highly conserved protein module of the innate immune system. Crit. Rev. Immunol. **24**:1–37.
72. **Kim YM, Kim EC, Kim Y.** 2011. The human lysyl oxidase-like 2 protein functions as an amine oxidase toward collagen and elastin. Mol. Biol. Rep. **38**:145–149.